CHEMICAL REVIEWS

Review

pubs.acs.org/CR

Water-Mediated Ion Pairing: Occurrence and Relevance

Nico F. A. van der Vegt,[*,†] Kristoffer Haldrup,[‡] Sylvie Roke,[§] Junrong Zheng,[∥,⊥] Mikael Lund,[#] and Huib J. Bakker[▽]

[†]Eduard-Zintl-Institut für Anorganische und Physikalische Chemie and Center of Smart Interfaces, Technische Universität Darmstadt, Alarich-Weiss-Strasse 10, 64287 Darmstadt, Germany

[‡]Physics Department, NEXMAP Section, Technical University of Denmark, Fysikvej 307, 2800 Kongens Lyngby, Denmark

[§]Laboratory for Fundamental BioPhotonics, Institute of Bioengineering, and Institute of Materials Science, School of Engineering, and Lausanne Centre for Ultrafast Science, École Polytechnique Fédérale de Lausanne, CH-1015 Lausanne, Switzerland

[∥]College of Chemistry and Molecular Engineering, Beijing National Laboratory for Molecular Sciences, Peking University, Beijing 100871, China

[⊥]Department of Chemistry, Rice University, 6100 Main Street, Houston, Texas 77005-1892, United States

[#]Division of Theoretical Chemistry, Department of Chemistry, Lund University, SE-22100 Lund, Sweden

[▽]FOM Institute AMOLF, Science Park 104, 1098 XG Amsterdam, The Netherlands

ABSTRACT: We present an overview of the studies of ion pairing in aqueous media of the past decade. In these studies, interactions between ions, and between ions and water, are investigated with relatively novel approaches, including dielectric relaxation spectroscopy, far-infrared (terahertz) absorption spectroscopy, femtosecond mid-infrared spectroscopy, and X-ray spectroscopy and scattering, as well as molecular dynamics simulation methods. With these methods, it is found that ion pairing is not a rare phenomenon only occurring for very particular, strongly interacting cations and anions. Instead, for many salt solutions and their interfaces, the measured and calculated structure and dynamics reveal the presence of a distinct concentration of contact ion pairs (CIPs), solvent shared ion pairs (SIPs), and solvent-separated ion pairs (2SIPs). We discuss the importance of specific ion-pairing interactions between cations like Li^+ and Na^+ and anionic carboxylate and phosphate groups for the structure and functioning of large (bio)molecular systems.

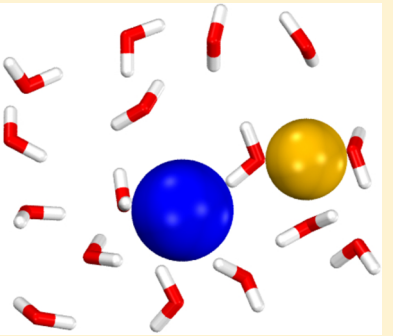

CONTENTS

1. INTRODUCTION

The structural and dynamical properties of water around ions in aqueous solution constitute a vast subject. Water is able to solvate an enormous range of different ionic species, ranging from the smallest, a solvated electron, to monatomic species, macromolecules such as proteins, and to ever-higher length scales. The complexity increases exponentially when one considers the interactions of multiple ions, from ion pairs to ion clusters, assemblies, and crystals. All these different ionic species have in common that there are still many fundamental open questions regarding their effect on the structure and dynamics of water and, in turn, how water influences the structure and dynamics of the ions. The work by Bernal and Fowler[1] is one of the first studies that directly addresses these questions from a structural point of view. This seminal article can be considered as a forerunner for many later studies, as it incorporates both state-of-the-art theoretical considerations and a range of, at that time, novel

Special Issue: Water - The Most Anomalous Liquid

Received: December 17, 2015

DOI: 10.1021/acs.chemrev.5b00742
Chem. Rev. XXXX, XXX, XXX−XXX

experimental techniques like Raman scattering, dielectric spectroscopy, and X-ray scattering.

Previous research on the structure of water around individual ions has been extensively reviewed, as in the now-classic article "Structure and dynamics of hydrated ions" from 1993 by Ohtaki and Radnai.[2] For monovalent cations, the distances to oxygen atoms of the water molecules in the first hydration shell reported by Ohtaki and Radnai are in the range from 1.9 Å (LiCl) to 3.2 Å (CsF), and where uncertainty estimates were available, they were typically in the range 0.01−0.03 Å. For di- and trivalent cations, the increase in Coulombic interaction and the smaller size of the cation leads to slightly shorter distances to the first hydration shell, ranging from 1.7 Å ($BeCl_2$) to 2.9 Å ($BaCl_2$) and from 1.9 Å ($AlCl_3$) to 2.2 Å [$Tl(ClO_4)_3$] for the di- and trivalent cations, respectively.

In the more recent review by Marcus in 2009,[3] it is commented that many studies of ion solvation require highly concentrated (>1 M) solutions that inevitably contain very little truly bulk water. Under these conditions, several studies that were focused on ion−water interactions also found evidence for ion−ion and, in some cases, ion−water−ion interactions. Indeed, at high salt concentrations, there is a significant probability for ion hydration shells to overlap, even if the ions are statistically distributed over the solution. However, there is now much evidence indicating that ions are not statistically distributed and that ion pairing is taking place at significantly lower concentrations through attractive interactions between the solvated ions of opposite charge. The attractive electrostatic potential between such species is significantly modified by the ease with which water can solvate ionic species varying in size and charge distribution, commonly referred to as hydrophobic and hydrophilic interactions. Further contributions to the potential arise from dipole−dipole interactions.

The 2009 review article on ion solvation by Marcus[3] provides a good overview of the experimental techniques that can be applied to study the hydration of ions. Complementing this work, a 2006 review of ion pairing by Marcus and Hefter[4] provides a comprehensive overview of different methods (conductivity, ultrasonic/dielectric relaxation, etc.) that have been used to study ion pairing. In this review, we will describe mainly recent (2006 until now) developments in the field of solvent-mediated ion pairing in water, often obtained with new experimental methods. These include scattering methods and nonlinear polarization-resolved and two-dimensional mid-infrared spectroscopic techniques. We will consider water-mediated ion pairing of simple oppositely charged ions and pay particular attention to the role and properties of water itself in such reactions. Therefore, although much work exists on ion pairing of like ions (e.g., ion pairing of the guanidinium ion with itself),[5,6] we will consider it only insofar as water plays an important role in the pair. Thus, in addition to contact ion pairs (CIP) where the ions are in direct contact, we will also describe recent results on solvent-shared ion pairs (SIPs) and solvent-separated ion pairs (2SIPs) where the ions are separated by one (SIP) or two (2SIP) water molecules. The systems and mechanisms discussed herein include ion pairs that rearrange on time scales comparable to that of the solvent. For simple ions such as Na^+ and Cl^-, a lifetime of 20 ps has been reported for the CIP in 0.5 *m* aqueous NaCl solution.[7] The lifetime of SIPs and 2SIPs is expected to be shorter. Clearly, a large variability exists in the strength and lifetime of ion pairing interactions for different systems. Even in systems with relatively weak ion-pairing interactions, the occurrence of SIPs and 2SIPs affects the dynamics of water, as well as thermodynamic solution properties, already at relatively low ion concentrations with a notable dependence on the specific ions involved. We will end this review by describing recent studies of ion pairing at interfaces. The behavior of ions at interfaces has been excellently reviewed recently,[8−10] showing the importance of ion pairing for atmospherically and biochemically important processes.

2. ION PAIRING IN AQUEOUS SOLUTIONS WITH STRONGLY HYDRATING CATIONS AND ANIONS

In recent years it has been demonstrated that formation of ion pairs and ion clusters in aqueous solution can be detected via far-infrared dielectric response of the salt solution and via infrared vibrational responses of water molecules and multiatom ions.[11−16] An ion pair consisting of a negative and positive ion has a large associated dipole moment that contributes to the dielectric response of the solution, provided that the ion pair remains intact for a time that is longer than the typical molecular reorientation time of the ion pair, typically >100 ps. The dielectric response of aqueous solutions can thus contain additional responses associated with different types of ion pairs, such as CIPs, SIPs, and 2SIPs.[11,12] Ion pairs have been observed with dielectric relaxation studies for solutions containing strongly hydrating cations and anions like Mg^{2+} and SO_4^{2-}.[12]

In Figure 1, real and imaginary parts of the dielectric function in the gigahertz domain of an aqueous solution of $MgSO_4$ are

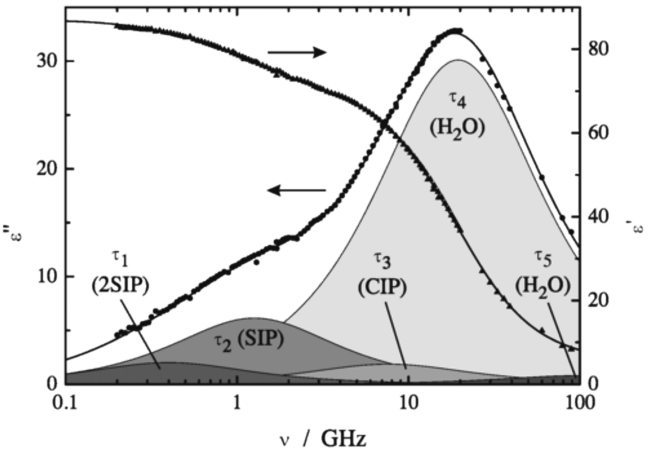

Figure 1. Dielectric permittivity, $\varepsilon'(\nu)$ (right vertical axis), and dielectric loss spectrum, $\varepsilon''(\nu)$ (left vertical axis), of a solution of 0.363 M $MgSO_4$ in water at 25 °C, showing contributions from various Debye processes to ε''. Solid lines are the sum of five processes. Reprinted with permission from ref 12. Copyright 2004 American Chemical Society.

presented. The spectrum contains a strong bulk water Debye mode at 20 GHz and a weaker water mode at a frequency of ∼110 GHz. In addition, the spectrum shows a pronounced response at lower frequencies that is assigned to different types of ion pairs (CIPs, SIPs, 2SIPs). These ion pairs differ in the number of hydration layers located between the Mg^{2+} cation and the SO_4^{2-} anion. With increasing number of water layers, the size of the ion-pair structure increases, resulting in a longer Debye reorientation time constant and a correspondingly lower frequency response in the ε'' spectrum. Similar and even stronger ion association effects have been observed in dielectric relaxation studies of solutions of $NiSO_4$, $CoSO_4$,[17] and $CuSO_4$.[18]

Formation of ion pairs and ion clusters can also be detected by their effect on the structure and dynamics of water molecules

DOI: 10.1021/acs.chemrev.5b00742
Chem. Rev. XXXX, XXX, XXX−XXX

contained in the shared hydration shell of the ions. The strong local electric field created by the positive and negative ion in an ion pair will align the water molecules between the ions, leading to a slowing down of the reorientation dynamics of the water molecules. This effect can be detected by probing the dipolar reorientation of water molecules with dielectric relaxation spectroscopy and by probing the reorientation of hydroxyl groups with polarization-resolved femtosecond mid-infrared spectroscopy.[13,14] In the latter technique, hydroxyl vibrations of water molecules are excited with a linearly polarized intense femtosecond mid-infrared pulse. The mid-infrared pulse preferentially excites hydroxyl vibrations that are oriented along the polarization of the pulse, meaning that the excitation will be anisotropic. The decay of this anisotropy due to reorientation of the water molecules is probed with time-delayed femtosecond infrared probing pulses with polarization directions parallel and perpendicular to the polarization of the infrared excitation pulse. Excitation of the hydroxyl stretch vibration thus serves as a label that enables real-time monitoring of the reorientation of water molecules.

In Figure 2A–C, the anisotropy of vibrational excitation is shown as a function of delay for three different salt solutions. All

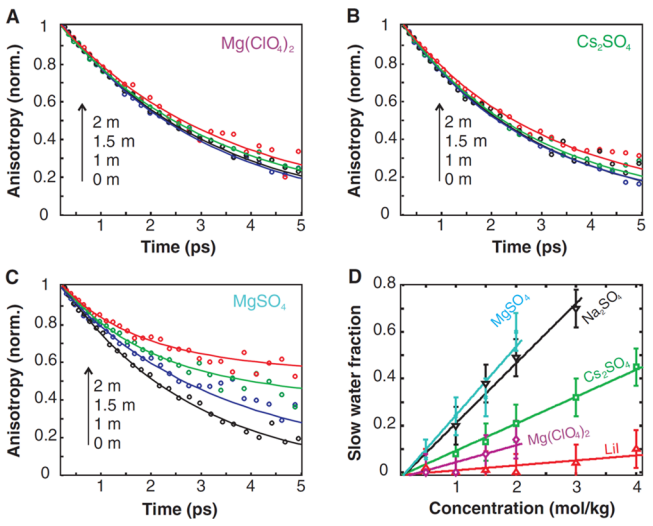

Figure 2. Normalized decay of the anisotropy R for (A) $Mg(ClO_4)_2$, (B) Cs_2SO_4, and (C) $MgSO_4$ at concentrations of 0, 1, 1.5, and 2 mol·kg^{-1}. Anisotropy decays are fitted with double exponentials with floating amplitudes and a time scale of 2.6 ps, as in bulk water, and a slow water time scale of 10 ps. (D) Fraction of slow water relative to bulklike water.[13] Reprinted with permission from ref 13. Copyright 2010 AAAS.

measurements show a decay component with a time constant of 2.6 ps, corresponding to the time scale of reorientation of bulk water. In addition, the anisotropy shows a much slower decay component with a time constant of ~10 ps. The amplitude of this component increases with increasing salt concentration, indicating that this component is associated with water molecules in the hydration shells of the ions. From the results of Figure 2A,B, it follows that Mg^{2+} and SO_4^{2-} slow down a small number of water molecules when these ions are combined with relatively weakly hydrating counterions like ClO_4^- and Cs^+. However, when Mg^{2+} and SO_4^{2-} are combined with each other, a large fraction of the water molecules is slowed down. Complementary dielectric relaxation data show that for $Mg(ClO_4)_2$ there are six slow water molecules ($N_p = 6$), associated with water molecules directly adjacent to the Mg^{2+} ion, and for Cs_2SO_4 there is one slow water molecule ($N_p = 1$), associated with a water molecule hydrating the SO_4^{2-} ion. For $MgSO_4$, $N_p = 18$, which is much larger than the sum of the water molecules being slowed down by $Mg(ClO_4)_2$ and Cs_2SO_4 (Figure 2). The results suggest that Mg^{2+} and SO_4^{2-} form solvent-separated ion pairs with a large number of confined water molecules between the two ions. In Figure 2D, the fraction of slow water is presented as a function of concentration for several salt solutions. For Na_2SO_4 a similar slow fraction is observed as for $MgSO_4$. The Na^+ ion will have a weaker interaction with SO_4^{2-} than Mg^{2+}, but this is compensated by the fact that Na_2SO_4 solutions contain two Na^+ ions per SO_4^{2-} ion. The femtosecond IR anisotropy-based observation of a large slow fraction of water molecules for Na_2SO_4 solution agrees with the results of a dielectric relaxation study.[11]

Ion pairing has also been studied in detail with molecular dynamics (MD) simulations.[19−24] Recently, work has appeared addressing ion pairing in relation to the specific nature of the ions and structural aspects of ion hydration.[25−34] In the MD simulations of Vila Verde and Lipowsky,[33] it was found that the interaction between Mg^{2+} and SO_4^{2-} ions leads to an additional slowing down of the reorientation of water molecules located between the ions, in agreement with experimental results. MD simulations of Stirnemann et al.[31] showed the presence of a strong nonadditive slowing-down effect of Na^+ and SO_4^{2-} ions on water reorientation, again in agreement with experimental observations. However, the slowing down was explained to be the result of a crowding effect that would be independent of the combination of ions. The combined slowing-down effect of cations and anions on water reorientation dynamics would thus occur only at high concentrations. However, the dielectric and femtosecond IR experimental work indicate that $MgSO_4$ and Na_2SO_4 do show specific ion-pairing interactions, leading to a combined slowing-down effect of cations and anions already at low salt concentrations.

3. ION PAIRING IN AQUEOUS SOLUTIONS WITH HALIDE ANIONS

3.1. Structural Characterization

Ion pairing and solvent-mediated ion pairing in water can be structurally characterized through the distribution of distances between ions and the structure of the hydration water. These parameters can be studied with techniques that are directly sensitive to structural properties, in particular methods relying on scattering that use short-wavelength X-ray and neutron radiation. Such methods include neutron scattering and hard X-ray wide- and small-angle scattering (WAXS/SAXS) as well as X-ray absorption spectroscopy (XAS), which is a highly sensitive probe of both local electronic and geometric structure around the absorbing atom and which can be combined with electron spectroscopy to yield further information.[35] The fundamentals of these techniques have recently been excellently reviewed by Bowron and Diaz Moreno.[36]

A drawback of scattering methods (both neutrons and X-rays, including extended X-ray absorption fine structure or EXAFS) is the inherently low information content of nondiffractive scattering.[37−39] Typically, only on the order of ten parameters can be determined by a (diffuse) scattering measurement, and as the scattering signal from even the simplest salt solutions arises from ten partial pair distribution functions,[36] the problem of structure determination is almost always underdetermined. Consequently there has been a strong drive to combine X-ray

DOI: 10.1021/acs.chemrev.5b00742
Chem. Rev. XXXX, XXX, XXX−XXX

methods with complementary sensitivities, for instance, X-ray scattering methods with X-ray absorption techniques. An important advantage of X-ray spectroscopic techniques over scattering-based techniques is that the former are intrinsically element-specific. As a result, even very dilute systems can be studied with XAS, but the interaction between electronic states and the X-ray probe in the measurement process may complicate the interpretation, as contributions arising from both electronic and geometric structure are overlaid, in particular near the absorption edges.

X-ray absorption fine structure (EXAFS) spectroscopy and pre-edge and near-edge (XANES) X-ray absorption have been combined to study the occurrence of ion pairing in $CaCl_2$ solutions in water.[40] The Ca K-edge EXAFS spectrum for 6 *m* $CaCl_2$ yielded no evidence for the formation of significant numbers of $Ca^{2+}-Cl^-$ contact ion pairs, even at such a high concentration. The water coordination number of Ca^{2+} was found to be 7.2 ± 1.2 molecules, and the average Ca−O distance was 2.437 ± 0.010 Å. This notion was confirmed by the pre-edge and near-edge (XANES) X-ray absorption data. The EXAFS spectrum for an even more concentrated (9.25 M $CaCl_2$) hexahydrate melt, however, did indicate the presence of some contact ion pairs. In the latter experiment, chemical specificity was obtained by utilizing isotope substitution, a methodology pioneered and developed by Enderby[41] and co-workers. In a neutron scattering study by Baydal et al.,[42] strong evidence was found for the presence of substantial amounts of $Ca^{2+}-OH_2-Cl^-$ solvent-shared ion pairs (SIPs), approximately 0.1 Cl^- ion around each Ca^{2+} at 6.4 M concentration and at a distance in the range from 4.6 to 5.6 Å. Taken together, $Ca^{2+}-OH_2-Cl^-$ SIPs seem to be far more prominent in $CaCl_2$ solutions than $Ca^{2+}-Cl^-$ contact ion pairs (CIPs), and the SIPs are most likely responsible for the unusual thermodynamic behavior of these solutions.

Arguably, the state-of-the-art in scattering-based investigations of ion pairs in solution is today dominated by such combined studies. These often include direct comparisons with high-level modeling or refinement of theoretical pair potentials through, for example, the empirical potential structure refinement (EPSR) methodology developed by Soper[43,44] and co-workers. A recent example of this approach, utilizing a combination of neutron and X-ray data, is the study by Diaz-Moreno et al.,[45] where the ion complexation and structure of ion pairs in aqueous $LaCl_3$ was described in detail. Specifically, at a concentration of 1 M, on the order of 1 Cl^- was found at a distance of 2.8 Å from each La^{3+} ion, forming an ion pair, with further Cl^- ions being present in the second solvation shell at a distance of ∼5 Å from the La^{3+} ions. As an alternative to the EPSR approach, structural models of ion pairing, notably radial distribution functions from molecular simulations, can be directly compared with the results of one or more scattering data sets, as shown for example in the neutron and X-ray study of Megyes et al.,[46] where $Na-NO_3$ CIPs were determined to have a distance of 3.50 Å at a concentration of 5.6 M and 3.49 Å at 7.5 M, in agreement with their MD simulations and with the average coordination number increasing from 1.35 to 2.1, and in the WAXS + EXAFS work by Pham and Fulton,[47] where Ru−Br CIPs as well as Ca−Cl CIPs and $Ca-H_2O-Cl$ SIPs were detected and their separations were determined (ion−ion distances of 2.71 and 4.98 Å, respectively, for the $CaCl_2$ system).

3.2. Far- and Mid-infrared Spectroscopy

Ion pairing of several di- and trivalent cations like Mn^{2+}, Ni^{2+}, Fe^{2+}, Fe^{3+}, and La^{3+} with halide ions has been investigated with high-precision far-infrared (terahertz) absorption spectroscopy in the frequency range 30−350 cm^{-1} (1−11.5 THz). With this technique, specific ion−water vibrations can be identified.[48−50] For $LaCl_3$ and $LaBr_3$, absorption of the ion vibrations shows a distinct nonlinear dependence on the concentration, indicative of the increasing formation of solvent-shared ion pairs with increasing salt concentration. The presence of distinct ion resonances shows that La^{3+} has only a local effect on the water structure, in spite of its high charge density. For $MnBr_2$, $NiCl_2$, and $MnCl_2$, evidence for the formation of contact ion pairs was found.[49] For acidified aqueous $FeCl_2$ and $FeCl_3$, a nonlinear concentration dependence of the absorption was found,[50] pointing to the progressive formation of chloro complexes of Fe(II) and Fe(III), that is, contact ion pairs. Properties of the chloro complex of Fe(III) have also been studied with soft X-ray photoelectron (PE) spectroscopy.[51] In this work it is observed that the Fe^{3+} cation shows a strong electronic-structure interaction with water molecules within the chloro complex. The effect of Cl^- ions on the Fe^{3+}−water interaction is comparatively weak.

In section 2 it was shown that the presence of ion pairing can be deduced from the combined effect of cations and anions on the dynamics of hydrating water molecules. This influence on the dynamics is not restricted to solutions of strongly hydrating ions like Mg^{2+} and SO_4^{2-}. Similar effects, albeit to a lesser extent, have been observed for alkali halide solutions.[52−55] In a recent femtosecond mid-infrared study, it was found that the nature of the alkali cation affects the reorientation of water in the hydration shell of the halide anion.[55] In this study, reorientation of water in the halide anion shells was observed to consist of a fast wobbling component with a time constant of ∼2 ps, which keeps the hydrogen bond to the anion intact, and a slow component with a time constant of ∼10 ps, which is assigned to reorganization of the hydration shell. The amplitude of the wobbling component was observed to depend on the nature of the cation: Na^+ decreases this amplitude more than K^+. This observation can be explained by the electric field exerted by the cation, which is larger for a small cation like Na^+ than for K^+. The electric field will align the static dipoles of the water molecules around the anion, thereby decreasing the cone angle over which the hydroxyl groups wobble.

3.3. Molecular Dynamics Simulations

Apart from solvent dynamics, ion pairing also affects the thermodynamics of aqueous electrolyte solutions, often giving rise to ion-specific changes in ion activities and related properties. Fennell et al.[56] studied the interaction of alkali cations and halide anions in water with computer simulations. By examining the relative depths of minima on the free energy surface of ion pairing, a good correlation was found with the "law of matching water affinities" of Collins:[57,58] small−small and large−large ion pairs should associate in water, while small−large pairs tend to stay separated. Hess and van der Vegt[26] and Ganguly et al.[28] provided an explanation for ion-specific trends in experimental osmotic coefficients in relation to the relative affinities of different ions to form CIPs and water-mediated SIPs/2SIPs in water. To relate ion pairing to osmotic properties of the specific salts, these authors used Kirkwood−Buff theory.[59] This theory has been increasingly applied in molecular simulations reported in recent years and has significantly contributed to the quality of

DOI: 10.1021/acs.chemrev.5b00742
Chem. Rev. XXXX, XXX, XXX−XXX

force-field models as well as to the understanding of relationships between ion pairing and thermodynamics. Some elements of this theory are briefly reviewed here.

Kirkwood–Buff theory relates solution structure to thermodynamic response functions through an analysis of particle number (density) fluctuations in open systems with constant chemical potentials of the solution components. The central quantity in this theory is the so-called fluctuation integral ("Kirkwood–Buff integral"), $G^V_{\alpha\beta}$, between component types α and β, which for finite volume V is defined as

$$G^V_{\alpha\beta} \equiv \frac{1}{V}\int_V\int_V [g_{\alpha\beta}(r_{12}) - 1]\,\mathrm{d}\mathbf{r}_1\,\mathrm{d}\mathbf{r}_2 = V\left[\frac{\langle N_\alpha N_\beta\rangle - \langle N_\alpha\rangle\langle N_\beta\rangle}{\langle N_\alpha\rangle\langle N_\beta\rangle} - \frac{\delta_{\alpha\beta}}{\langle N_\alpha\rangle}\right] \quad (1)$$

In eq 1, N_α is the number of molecules of component α, $\delta_{\alpha\beta}$ is the Kronecker delta, $g_{\alpha\beta}(r)$ is the pair correlation function between $\alpha\beta$ pairs, $r_{12} = |\mathbf{r}_1 - \mathbf{r}_2|$, and angle brackets denote an average in the grand-canonical ensemble. In the limit $V \to \infty$, the integral in eq 1 reduces to

$$G^\infty_{\alpha\beta} = 4\pi\int_0^\infty [g_{\alpha\beta}(r) - 1]r^2\,\mathrm{d}r \quad (2)$$

Many thermodynamic properties of multicomponent systems follow from the Kirkwood–Buff integrals $G^\infty_{\alpha\beta}$[60] which can be calculated from molecular simulation trajectories, provided that appropriate methods are used to account for finite size effects.[61,62] In recent years, Kirkwood–Buff theory has been used in the molecular simulation community to optimize and validate empirical pair potentials for electrolyte solutions against available experimental data.[26,63−68] In these applications, the solvated cations and anions are usually treated as indistinguishable species and thermodynamic data are derived via Kirkwood–Buff formulas for binary systems.[60] This assumption, however, is not strictly required. Therefore, individual ion properties can also be assessed by application of Kirkwood–Buff theory.[69]

The Kirkwood–Buff relationship for the osmotic coefficient, ϕ, here described for a binary solution with water (W) and salt (S), is of particular interest in relation to ion pairing:

$$\left(\frac{\partial[\rho_S(\phi - 1)]}{\partial\rho_S}\right)_{P,T} = \frac{-(\Delta N_{SS} - \Delta N_{WS})}{1 + (\Delta N_{SS} - \Delta N_{WS})} \quad (3)$$

In eq 3, ρ_S is molar salt concentration, $\Delta N_{SS} = \rho_S G_{SS}$ and $\Delta N_{WS} = \rho_S G_{WS}$ are salt–salt and water–salt excess coordination numbers, respectively; P is pressure, and T is temperature. The quantity $RT\rho_S(\phi - 1)$ represents the contribution of effective ion–ion interactions to the osmotic pressure; that is, it is the measured osmotic pressure minus the van't Hoff (ideal gas) pressure of the ions. Equation 3 is exact and demonstrates that an unbalance between *excess* ion pairing (ΔN_{SS}) and *excess* ion hydration (ΔN_{WS}) leads to changes of ϕ with salt concentration ρ_S. Such changes in ϕ, which can be related to the accompanying changes in mean ionic activity coefficient by means of a Gibbs–Duhem relationship, are ion-specific and, by application of eqs 2 and 3, can be related to ion–ion and ion–water correlations.

The osmotic coefficients ϕ and their derivatives (eq 3) of 1 M aqueous alkali halide solutions (X^- = Cl^-, Br^-, I^-) vary with ρ_S in the order LiX > NaX > KX > RbX > CsX.[70] Molecular simulations of these systems with accurate, Kirkwood–Buff-derived empirical force field models have shown that the above series can be explained by considering the quantity ΔN_{SS}, in particular, the differences in cation–anion pairing propensities in CIP, SIP, and 2SIP states that contribute to it.[26,28] Hence, the quantity ΔN_{SS}, which can be written as $\Delta N_{CIP} + \Delta N_{SIP} + \Delta N_{2SIP} + C$ (where C is an ion-unspecific constant), increases in the order LiX < NaX < KX < RbX < CsX, which can be explained in terms of differences in CIP, SIP, and 2SIP contributions. These differences cause ion-specific variations of ϕ and are dominated by CIPs for alkali halides (see Figure 3). Therefore, the magnitude of contact ion pairing determines the differences in osmotic activities among alkali halides.

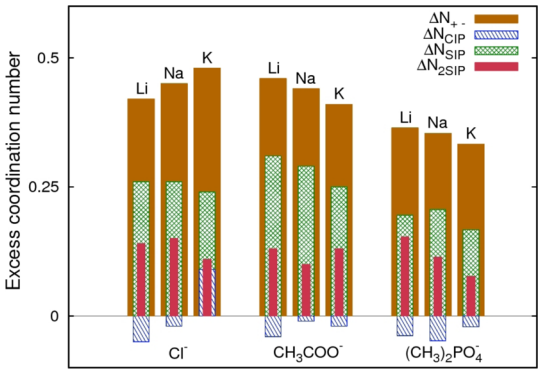

Figure 3. Excess cation–anion coordination numbers in alkali chloride, alkali acetate, and alkali dimethyl phosphate aqueous solutions (1 *m* salt, 298 K). ΔN_{+-} is the total excess and ΔN_{CIP}, ΔN_{SIP}, and ΔN_{2SIP} are the contributions of contact, solvent-shared, and solvent-separated ion pairs to the total excess, respectively. Differences in the occupation of CIP states determine the ion-specific changes in salt osmotic activities of alkali chlorides. For alkali acetate and alkali dimethyl phosphate, ion-specific changes in salt activities are due to changes in the occupation of SIP and 2SIP states, respectively. Reprinted with permission from ref 28. Copyright 2011 American Chemical Society.

4. ION PAIRING IN AQUEOUS SOLUTIONS WITH CARBOXYLATE AND PHOSPHATE GROUPS

Contrary to the alkali halides, ion-specific variations in the osmotic activities of carboxylate and phosphate salts are determined by SIPs and 2SIPs, respectively (Figure 3). This leads to a reversal in the Hofmeister ion series of the osmotic coefficient. It is interesting to note that, for Li^+, the above role of SIPs was postulated in early work by Robinson and Harned.[71] They observed that a reversal in the order of salt activity curves, compared to chlorides and bromides, is found in the case of anions that are strong proton acceptors. These anions are usually derived from weak acids. In particular, for Li^+, water oxygens strongly coordinate the positive ion while protons in these water molecules are repelled from the hydration sheath and form linkages with any proton acceptor, such as acetates, in their vicinity.

Ion-pairing effects of cations and anions on the dynamics of water have also been observed for alkali and alkaline-earth cations interacting with anionic carboxylate and phosphate groups.[72−77] Figure 4a presents the slow fraction of water in solutions of different formate salts, measured with polarization-resolved femtosecond mid-infrared spectroscopy. Figure 4b shows the corresponding hydration numbers, as determined from the slopes in Figure 4a. The number of slowed-down water molecules increases in the sequence $Cs^+ < K^+$, $NH_4^+ < Li^+ < Na^+$. The combination of Na^+ and $HCOO^-$ leads to a strong

DOI: 10.1021/acs.chemrev.5b00742
Chem. Rev. XXXX, XXX, XXX−XXX

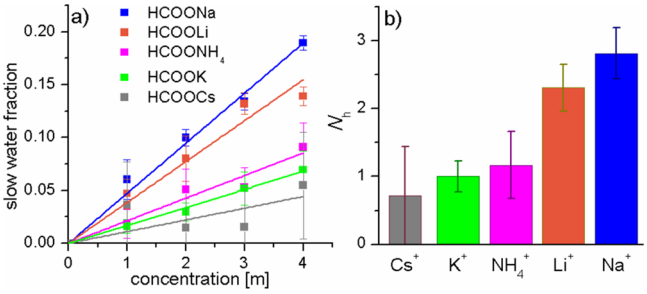

Figure 4. (a) Fraction of slow water as a function of concentration for different formate salts. Points originate from biexponential fits to measured anisotropy curves, and lines are obtained from linear fits to these points. (b) Hydration number, N_h, for different formate salts. Reprinted with permission from ref 77. Copyright 2013 PCCP Owner Societies.

slowing down of the reorientation dynamics of ~3 water molecules. This slowing down is not observed if Na^+ is combined with a weakly hydrating anion like I^-, which implies that the slowed-down water molecules cannot be attributed to the hydration shell of an isolated Na^+ ion.

The cooperative effect of the carboxylate group and particular alkali cations likely finds its origin in the formation of solvent−shared ion pairs. Water molecules contained between oxygen atoms of the carboxylate anion and the cation will show different reorientation dynamics from water molecules in bulk liquid water. Similar effects of ion pairing on the dynamics of water have been observed for phosphate headgroups of phospholipids.[76] Strongly hydrating cations like Na^+ and Ca^{2+} form a hydration complex or solvent-shared ion pair with the phosphate headgroup. For weakly hydrating cations like K^+ and NH_4^+, such ion pairs are not observed.

Figure 3 shows excess cation−anion ion pairs for alkali acetate salts. For the carboxylate anion, the total excess number of ion pairs (CIPs + SIPs + 2SIPs) follows $Li^+ > Na^+ > K^+$, which implies that the order is reversed compared to alkali chloride salts. This reversal results from changes in the excess numbers of SIPs (for acetate) and 2SIPs (for dimethyl phosphate). The SIP state of sodium acetate has greater thermodynamic stability than the SIP state of potassium acetate, the magnitude of which is determined by subtle differences in Coulombic ion−ion and hydrogen-bond interactions. This finding agrees with results from femtosecond mid-infrared experiments that also demonstrated the presence of a larger fraction of slow water for solutions of sodium formate than for solutions of potassium formate. Interestingly, both MD simulations[26] and femtosecond mid-infrared results found the fraction of SIPs (not to be confused with the excess coordination number of SIPs in Figure 3) to be larger for the combination of Na^+ and $-COO^-$ than for the combination of Li^+ and $-COO^-$. This result is surprising because the Li^+ ion possesses higher charge density than Na^+. The MD simulations also find the fraction of CIPs to be higher for Na^+ and $-COO^-$ than for Li^+ and $-COO^-$. A similar (unexpected) order of the fraction of CIPs formed by Na^+ and Li^+ is found in an X-ray absorption spectroscopy study of aqueous solutions of acetate.[78]

Figure 5 presents X-ray absorption (XA) spectra of a series of 1 M acetate aqueous solutions with Li^+, Na^+, K^+, and NH_4^+ as the counterions. For comparison, the XA spectrum of pure water is also shown. The O 1s XA spectra of pure water and the aqueous solutions are dominated by so-called pre-edge absorption at 535 eV, main-edge absorption at 538 eV, and post-edge absorption at

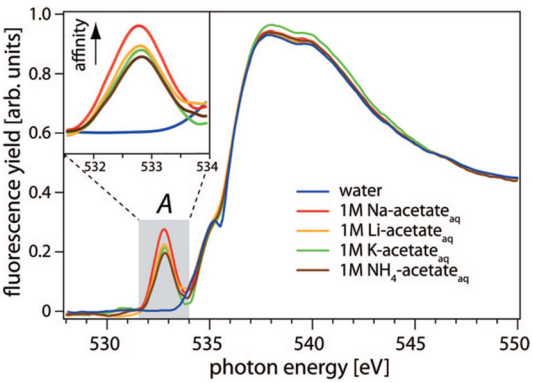

Figure 5. X-ray absorption spectra of the oxygen K-edge for solutions of acetate and different cations. (Inset) Region of the peak at 532.8 eV that corresponds with oxygen atoms of acetate. Reprinted with permission from ref 78. Copyright 2008 American Chemical Society.

540 eV. Spectra of acetate solutions contain an additional absorption peak A at 532.8 eV that is associated with the $-COO^-$ group of acetate. The intensity of peak A increases in the sequence $NH_4^+ < K^+ < Li^+ < Na^+$. This increase in intensity results from the withdrawal of electrons from the carboxylate group by a nearby cation. Hence, the observed increase in intensity of peak A can be explained by an increase in the fraction of CIPs in the sequence $NH_4^+ < K^+ < Li^+ < Na^+$. X-ray absorption spectra thus show that the fraction of CIPs is larger for Na^+ than for Li^+, in agreement with MD simulations.[26] This cationic ordering agrees well with Collins' law of matching water affinities[57,58] since Na^+ matches best the hydration enthalpy of the $-COO^-$ ion, followed by Li^+, K^+, and NH_4^+. A somewhat different explanation is that the Na^+ ion, in view of its size, has a better fit to the carboxylate group and its first hydration layer than the Li^+ ion. This latter explanation agrees with the fact that Figure 3 shows that, in spite of the higher fractions of CIPs and SIPs of Na^+, the overall ion-pairing probability is higher for Li^+, due to the significantly higher fraction of 2SIPs of the Li^+ ion.

Figure 6 shows radial distribution functions of cations (Li^+, Na^+, K^+) with nonmethylated oxygen in $(CH_3)_2PO_4^-$, calculated from MD simulations.[28] While direct interactions of sodium and potassium with the phosphate oxygen are observed, the peaks

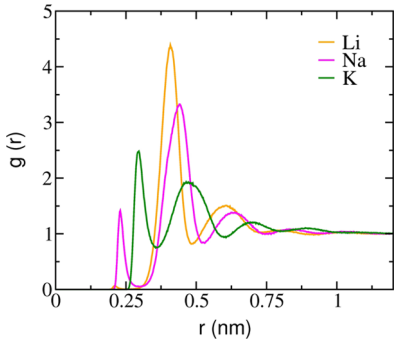

Figure 6. Calculated cation−oxygen (dimethyl phosphate) radial distribution functions at 1 *m* salt concentration and 298 K.[28] Dominant structural correlations are observed at distances corresponding to SIP and 2SIP states; the peak heights corresponding to these states follow $K^+ < Na^+ < Li^+$. While the CIP state is hardly visible for Li^+, CIP peaks are observed for Na^+ and, more prominently, for K^+. Reprinted with permission from ref 28. Copyright 2011 American Chemical Society.

DOI: 10.1021/acs.chemrev.5b00742
Chem. Rev. XXXX, XXX, XXX−XXX

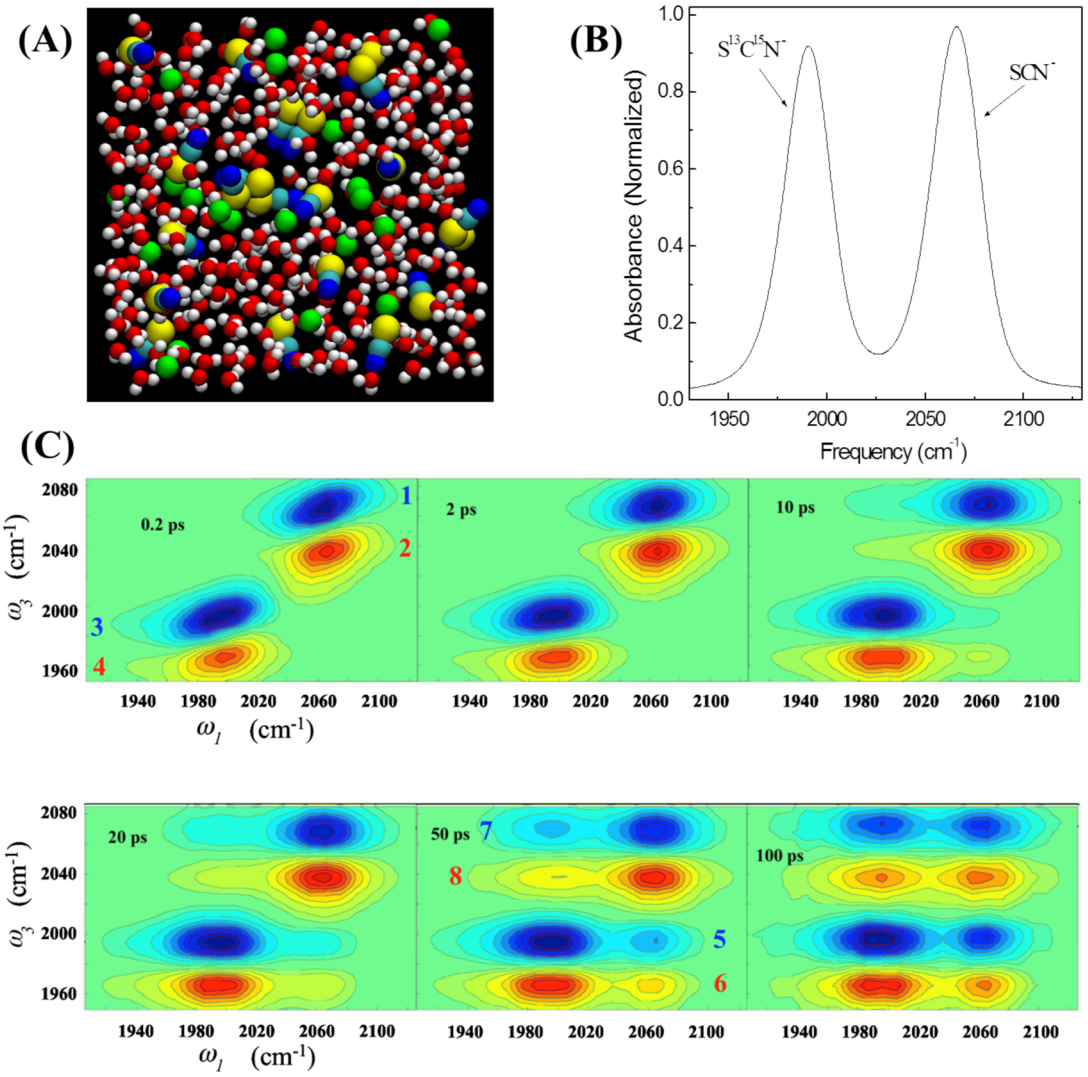

Figure 7. (A) Snapshot of 1.8 M KSCN aqueous solution from MD simulation: O (red), H (white), C (light blue), N (dark blue), K (green), and S (yellow). Some water molecules are removed to better display the cluster structure. (B) FT-IR spectrum of the CN and $^{13}C^{15}N$ stretches of SCN^- and $S^{13}C^{15}N^-$ of a 10 M KSCN/$KS^{13}C^{15}N$ (1/1) aqueous solution. (C) Time dependence of 2D-IR spectrum of 10 M solution. As T_w increases, the off-diagonal peaks grow because of vibrational energy exchange between SCN^- and $S^{13}C^{15}N^-$. Reprinted with permission from ref 15. Copyright 2011 National Academy of Sciences.

corresponding to solvent-separated distances are significantly more pronounced.

Ion-pair formation has also been studied as a function of temperature. For alkali acetate solutions, the ratio of SIPs over CIPs in alkali acetate solution is calculated to be larger at lower temperatures (relative to 298 K), and to be smaller at high temperature.[79] This observation indicates that formation of the SIP state is associated with a smaller enthalpy change than formation of the CIP state. Enthalpy of the SIP states of Li^+, Na^+, and K^+ with acetate is furthermore seen to be lower than that of double-solvent-separated configurations.

5. FORMATION OF ION CLUSTERS IN WATER

The properties of aqueous solutions of strong electrolytes deviate from those of ideal solutions already at extremely low concentrations ($<10^{-5}$ M). The deviations were generally believed to be caused by attraction and repulsion of the ions, leading to the development of the Debye–Hückel theory.[80,81] However, this theory fails at higher concentrations, and the formation of ion pairs containing two ions of opposite charge has been proposed to be primarily responsible for this failure.[82,83] MD simulations also suggested that clusters with more than two ions may exist and that these clusters could be a major factor causing the nonideality of solutions and could form nucleation sites for crystal growth at medium or high concentrations.[84−87] For unsaturated solutions of complex salts or neutral species, the presence of large clusters has been experimentally demonstrated by use of various techniques, such as neutron scattering, light scattering, and Raman spectroscopy, albeit with several assumptions in interpretation of the measurements.[88−92] For solutions with simple ions (Figure 7A), MD simulations predict the presence of small clusters containing only a few ions. Detection of these small clusters with the usual tools for probing structures in liquids, X-ray or neutron diffraction[93] or dynamic light scattering,[86,94] is extremely challenging because the contribution of ion–ion correlations to the total scattering pattern is small compared to contributions from water–water and water–ion interactions.[86]

DOI: 10.1021/acs.chemrev.5b00742
Chem. Rev. XXXX, XXX, XXX−XXX

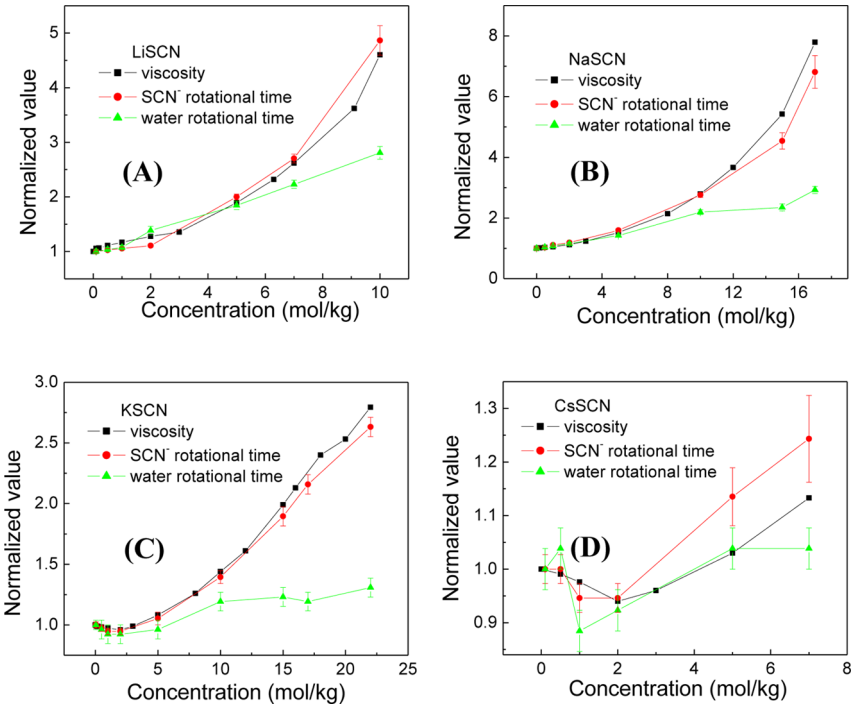

Figure 8. Normalized viscosities and SCN^- and water (OD) rotational time constants for aqueous solutions of (A) LiSCN, (B) NaSCN, (C) KSCN, and (D) CsSCN as a function of salt concentration. Viscosities are normalized to the value for pure water of 0.97 cS. Water rotational time constants are normalized to the value 2.6 ps of pure water. and rotational time constants of SCN^- are normalized to the value 3.7 ps observed for 0.1 M MSCN.[95] Adapted with permission from ref 97. Copyright 2013 American Chemical Society.

5.1. Aggregation in Solutions of SCN^- Ions

Very recently, ion pairing and clustering in aqueous solutions of monocharged ions have been observed with vibrational energy transfer and molecular rotational measurements based on ultrafast IR methods.[14−16,95−100] Multiatom ions like SO_4^{2-} and SCN^- possess vibrational resonances that can be excited and probed with femtosecond mid-infrared laser pulses. For this type of ions, the formation of ion pairs and ion clusters can be studied by monitoring the rate of near-resonant vibrational energy transfer between the ions.[15,16] This energy transfer relies on the (Förster) dipole−dipole coupling of the vibrations and thus strongly depends on the distance r between the ions, according to r^{-6}. Hence, if ions are at close distance, forming ion pairs or clusters, this will lead to a high rate of near-resonant energy transfer. The rate of energy transfer between the ions can be monitored with femtosecond two-dimensional infrared (2D-IR) spectroscopy, where different ions can be distinguished by using isotopic mixtures, for example, SCN^- and $S^{13}C^{15}N^-$.[15] Alternatively, Auger electron spectroscopy may also report on ion pairing in aqueous solution, in that changes in the local environment around water can be related to simultaneous action of a cation and an anion.[35]

The vibrational energy transfer method involves measurement of the rate of energy transfer between two vibrational modes located on two ions.[15,96] This energy transfer relies on dipole−dipole coupling of the two vibrational modes and thus strongly depends on the distance between the ions. Hence, the rate of energy transfer can be related to the distance between two ions.[16,95] In aqueous solutions, the distance between two ions is typically much larger than the length of a chemical bond, and the vibrational coupling between two vibrational modes on two different ions is typically smaller than the vibrational dephasing line widths of the modes.[16,95] As a result, energy transfer can be described in the weak coupling limit by use of point dipoles, leading an energy transfer rate constant k that strongly decreases with increasing distance r, following $k \propto r^{-6}$.[16,95] In general, water-solvated ions and water solvent-separated ion pairs (SIPs) have much larger interionic distances than contact ion pairs (CIPs). Therefore, the vibrational energy transfer method primarily probes CIPs.

The vibrational energy transfer method has been intensively used to study ion clustering in aqueous solutions of thiocyanate (SCN^-) anions and various cations at different concentrations.[15,16,95−99] Figure 7B shows the Fourier transform infrared (FT-IR) spectrum of CN and $^{13}C^{15}N^-$ stretches of SCN^- and $S^{13}C^{15}N^-$ in 10 M potassium thiocyanate (KSCN/$KS^{13}C^{15}N$ = 1/1) aqueous (D_2O) solution.[15] Isotope labeling shifts the CN stretch frequency from 2066 cm^{-1} (SCN^-) down to 1991 cm^{-1} ($S^{13}C^{15}N^-$). In Figure 7C, the 2D-IR vibrational spectrum of these modes is presented (for 10 M solution). The two diagonal-peak pairs labeled 1, 2 and 3, 4 represent anions that have not yet transferred their energy. At a very short waiting time, T_w = 200 fs, at which negligible vibrational energy exchange has occurred, the spectrum contains only diagonal peak pairs. Peaks 1 and 2 represent 0−1 and 1−2 transitions of the CN vibration of SCN^-, and peaks 3 and 4 correspond to 0−1 and 1−2 transitions of the $^{13}C^{15}N^-$ vibration of $S^{13}C^{15}N^-$. With increasing T_w, an increasing amount of vibrational energy is transferred between the two anions. At longer waiting times, the cross-peak pairs labeled 5, 6 and 7, 8 begin to grow. These new peaks arise from the transfer of vibrational energy. Vibrational energy transfer from SCN^- to $S^{13}C^{15}N^-$ produces peaks 5 and 6. These peaks are located at excitation frequency ω_1 of 2066 cm^{-1}, which corresponds to the 0−1 transition frequency of the CN stretch of SCN^-, and detection frequencies ω_3 of 1991 and 1966 cm^{-1} that correspond to 0−1 and 1−2 transition frequencies of the $^{13}C^{15}N^-$ stretch

DOI: 10.1021/acs.chemrev.5b00742
Chem. Rev. XXXX, XXX, XXX−XXX

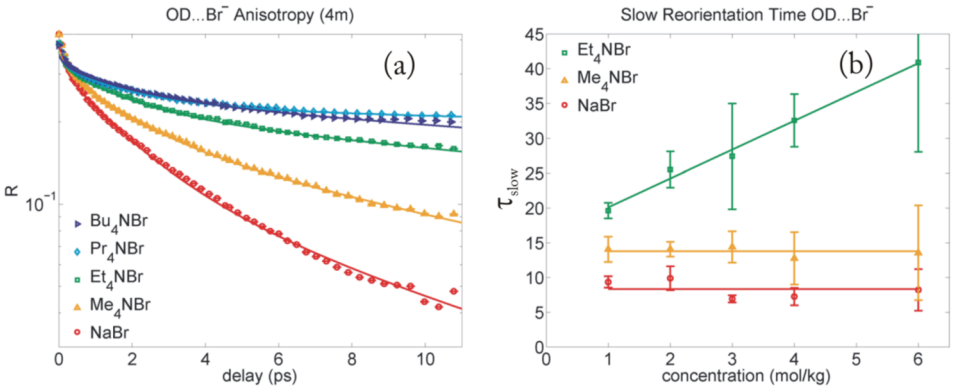

Figure 9. (a) Anisotropy of O−D stretch vibrational excitation in the hydration shell of Br^- ion as a function of time delay for different A_4NBr salts. For comparison, anisotropy measured for a solution of NaBr is also shown. (b) Time constant of the slow decay component of anisotropy dynamics. Reprinted with permission from ref 14. Copyright 2013 American Chemical Society.

vibration of $S^{13}C^{15}N^-$, respectively. Likewise, the peaks labeled 7 and 8 are produced by energy transfer from $S^{13}C^{15}N^-$ to SCN^-. A simultaneous fit of time-dependent intensities of diagonal peaks and cross peaks shows that more than 95% of the anions are located in ion clusters. Energy transfer from SCN^- to surrounding $S^{13}C^{15}N^-$ anions has a time constant of 115 ps.[15] The size of the clusters can be estimated by measuring the anisotropy dynamics of vibrational excitations. It is found that in this 10 M solution the ion clusters contain at least 18 anions. By the same approaches, ion clusters in the KSCN aqueous solutions are found to be disrupted by addition of ions and molecules with different properties.[98,99] Fewer and smaller clusters are found in more dilute solutions. At 1 M, only about 20−30% of the ions form clusters with an average size of two to three anions. More and larger clusters are formed in solutions with larger cations ($Cs^+ > K^+ > Na^+ > Li^+$). This trend follows the empirical law of "matching water affinities":[56−58,101] small−small and large−large ion pairs easily associate, while small−large ion pairs readily dissociate. SCN^- is large and polarizable and therefore more readily binds with the large and polarizable Cs^+ than the small Li^+. The distance between two thiocyanate anions in the clusters in the solutions is determined to be the same as the shortest distance between two anions in the KSCN crystal.[16,95] The rotational time constant of the anion in 10 M solution is also the same as that in the crystal.[15,16] In spite of these similarities between ion clusters and the crystal, MD simulations, FT-IR, and anisotropy measurements all suggest that the structures of ion clusters in aqueous solution are meltlike (molten salt) rather than crystal-like.[16,97]

The experiments described above do not provide direct information on the cations, because alkaline cations have no vibrational signal. Direct information on the clustering behavior of other, more complex cations can be obtained by studying vibrational energy transfer between anion and cation for solutions of NH_4SCN.[96] This study shows that the clusters formed in 4 M NH_4SCN aqueous solution have a cation/anion ratio of approximately 1.[96] The occurrence of ion pairing and clustering in aqueous solutions can also be inferred from concentration-dependent viscosity and molecular rotation measurements.[14,97,99,102,103] In molecular rotation measurements, reorientation of the water molecules or the ions is probed via dynamics of the anisotropy of the nonlinear signal resulting from excitation of the hydroxyl stretch vibration of the water molecules or a vibrational mode of the ions, for example, the CN stretch of SCN^-. Decay of the anisotropy directly reflects reorientation of water molecules or ions in the solution. Because water molecules have different frequencies in different environments, the technique allows for a distinction between the reorientation dynamics of water molecules forming hydrogen bonds to other water molecules (in the bulk and in the cation hydration shell) and the dynamics of water molecule forming hydrogen bonds to a halide anion. As displayed in Figure 8C, with increasing ion concentration, the viscosity of the solution first decreases slightly and then (from about 2 M) increases gradually to about 2.8 times that of pure water at saturation. Relative change of the rotational time constant of the SCN^- anion is almost identical to that of the viscosity. However, in the same solutions, the rotational behavior of water is quite different. At saturation, the rotation of water slows down for about 35%, significantly smaller (~270%) than that of SCN^-. The different concentration-dependent rotational dynamics of water and SCN^- can be explained only with ion clustering.[97,99] At low concentrations, most ions are solvated by water. Because both K^+ and SCN^- have weak interactions with water, the average rotation of water and SCN^- becomes faster with more ions present in solution. However, at higher concentrations, a substantial fraction of the ions will be involved in ion clusters, and the rotation of SCN^- slows down significantly. The formation of ion clusters does not affect water rotational dynamics significantly, as most water molecules are located outside the cluster, in the "bulk" state. The difference in SCN^- and water dynamics is also observed in other solutions of alkaline thiocyanate, as displayed in Figure 8. Figure 8 also shows that, in a solution with a smaller cation, the viscosity is larger and concentration-dependent rotational changes of the anion and water are more similar. This stronger similarity can be explained from the fact that a small cation has a stronger interaction with water,[97,104] which also leads to multiple time scales for both water and anion reorientation.[97] The multiple time scales of reorientation evolve to a single time scale when the size of the cation increases.[97] Rotational times in Figure 8 are average time constants with single-exponential fits.[97]

5.2. Aggregation in Solutions of Tetra-*n*-alkylammonium Ions

Ion aggregation is also observed for aqueous solutions of tetra-*n*-alkylammonium ions $[N(C_nH_{2n+1})_4^+]$.[14] It is well-known that molecules containing hydrophobic groups can form aggregates in aqueous solution, especially at high concentrations. For ions containing hydrophobic groups, aggregation is less obvious, in view of the attractive Coulomb interactions with water molecules

DOI: 10.1021/acs.chemrev.5b00742
Chem. Rev. XXXX, XXX, XXX−XXX

and the repulsive interaction between ions of the same charge. Tetra-*n*-alkylammonium (A_4N^+) ions are ideal to study the aggregation of hydrophobic ions, as these salts can be dissolved in liquid water up to high concentrations, and the hydrophobic interaction can be tuned by changing the length of the alkyl chains.

The properties of A_4N^+ dissolved in water have been studied with several techniques, including MD simulations,[105,106] dielectric relaxation,[107] small-angle X-ray scattering (SAXS),[108] and polarization-resolved femtosecond infrared spectroscopy.[14] With the latter technique it is possible to distinguish the dynamics of water molecules forming hydrogen bonds to, for example, Br^- anions from the dynamics of water molecules forming hydrogen bonds to other water molecules. Figure 9a presents the anisotropy dynamics of water molecules in the hydration shell of Br^- anions, measured for solutions of different A_4NBr salts.

It is seen that the dynamics of water molecules forming hydrogen bonds to the Br^- anions strongly slows down with increasing length of the alkyl chains. The anisotropy dynamics are decomposed in a fast component with a time constant of ∼2 ps and a slow component, for which a time constant was fitted for each concentration. The fast decay process is associated with the wobbling motion of water molecules that keep the hydrogen bond to the anion intact. As the anion restricts the wobbling motion to a certain angle, this process does not lead to a full decay of anisotropy. Complete decay of anisotropy involves the much slower process of rotational diffusion of the complete solvation structure or of the water molecules over the anionic surface.[55]

The results of Figure 9a show that the presence of hydrophobic cations leads to a severe retardation effect in the anisotropy dynamics of the hydration shell of the Br^- anion. In Figure 9b, the time constant of the slow reorientation process is plotted as a function of concentration. The results of Figure 9b show that, for Et_4NBr, the time constant of the slow reorientation component increases from 20 ps at 1 M to more than 40 ps at 6 M. The slowing down of water reorientation with increasing concentration for solutions of Et_4NBr points at the formation of domains in which Br^- anions and Et_4N^+cations cluster together, with a restricted number of water molecules in between. These confined water molecules will show very slow reorientation, as has also been observed for reversed micelles[109] and ionic liquids.[110] For Pr_4NBr and Bu_4NBr, the time constant of the slow reorientation component in the hydration shell of Br^- is >40 ps, already at low concentrations, somewhat larger than the values obtained from dielectric relaxation studies for concentrations of these salts lower than 3 *m*.[107] In this latter study, the reorientation time of water molecules hydrating Pr_4N^+ or Bu_4N^+ was found to become exponentially slower for concentrations larger than 2.2 and 1.7 M, respectively. The large reorientation time constant of Pr_4NBr and Bu_4NBr solutions suggests that the formation of aggregated ion clusters already occurs at the lowest concentrations investigated. The affinity of large halide anions for alkylammonium cations was also observed in MD simulations[27] as well as with NMR spectroscopic measurements of quadrupolar relaxation rates.[111,112] In the SAXS study by Huang et al.,[108] a similar crossover in the aggregation of tetraalkylammonium ions was observed. In this study, it was also found that Pr_4N^+ or Bu_4N^+ showed much stronger aggregation than Me_4N^+ and Et_4N^+. The authors established a crossover point between 4.4 and 5 Å for solute size.

For Me_4NBr, the slow reorientation time constant has a constant value of 15 ps up to a concentration of 6 M, indicating that aggregation and confinement do not play a significant role for solutions of Me_4NBr. Apparently, for the Me_4N^+ cation the repulsive Coulomb interactions are strong enough to prevent large aggregation. However, from comparison of time constants, ∼15 ps for Me_4NBr and ∼10 ps for NaBr, it is clear that the hydrophobic nature of Me_4N^+ still has an effect on the reorientation of water molecules hydrating the Br^- anion. The difference between Me_4NBr and NaBr suggests that Me_4N^+ may form some solvent-separated ion pairs with Br^-, as has also been proposed from dielectric relaxation studies and MD simulations.[27,107] This result agrees with the results of MD simulations of KSCN and NaSCN solutions.[97,104] In these simulations the reorientation dynamics of water molecules inside solvent-separated ion pairs and clusters is also found to be slower than in bulk liquid water.[78,84]

In the case where one alkyl tail of the tetraalkylammonium ion is much longer than the other three alkyl groups, the ion forms a cationic surfactant where the long aliphatic tail forms the apolar part and the remaining trialkylammonium part is the cationic headgroup. These ions are referred to as C_nTA^+ ions, where C_n indicates an aliphatic tail of length *n* and TA^+ denotes a Me_3N^+ or Et_3N^+ headgroup. C_nTA^+ ions support the formation of micelles and reverse micelles. In a recent Raman spectroscopic study, hydration of C_nTA^+ surfactants with a Me_3N^+ headgroup and various aliphatic chain lengths ($n = 7-12$) was investigated both below and above the critical micelle concentration.[113] It was found that water penetrates significantly into the micelle interior, well beyond the first few carbons adjacent to the headgroup. These results indicate that the micelle surface is highly corrugated, containing hydrated nonpolar cavities whose depth increases with increasing surfactant chain length. C_nTA^+ ions are combined with an anion, usually Cl^- or Br^-. In the same Raman spectroscopic study, evidence was found that benzene molecules near the micelle surface interact both with the Me_3N^+ head groups and with the Br^- counterions, showing that Me_3N^+ and Br^- probably form (solvent-separated) ion pairs at the micelle surface.

As an alternative technique, NMR spectroscopy can be used to detect ion pairs in aqueous solution. For example, the pairing of alkali metal ions with silicate anions is stronger for larger cations, which tend to attract silicate oligomers.[114] This observation contradicts the Bjerrum ion-pairing model[115] where pair formation decreases with cation size, and it has been argued that this is due to increased polarizability of the larger cations.[114]

6. ION PAIRING AT INTERFACES

Measurement of the interactions between ions near surfaces requires experimental techniques that are highly surface-specific. Such a technique is surface-enhanced Raman spectroscopy. With this technique, Perera et al.[116] found evidence for ion pairing for a large variety of salt solutions, including salts with Cl^-, Br^-, and I^- as anions and Li^+, Na^+, K^+, 3-bis(3-butylimidazolium)benzene^{2+}, and 1-allyl-3-methylimidazolium$^+$ as cations.

Ions can also form ion pairs with charged groups located at surfaces, and this interaction can have a strong effect on the character of the surface, for example, hydrophilic or hydrophobic. Ion pairs are often formed between dissolved cations and surface-bound anionic groups like sulfate, carboxylate, and phosphate. One technique to probe these interactions is the highly surface-specific technique of surface sum-frequency generation (SFG). In this technique an infrared and a visible pulse are combined to

DOI: 10.1021/acs.chemrev.5b00742
Chem. Rev. XXXX, XXX, XXX−XXX

generate their sum frequency. This process is allowed only if the system under study lacks inversion symmetry, which for aqueous solutions is the case only at the surface. Hence, for aqueous solutions the sum-frequency light is generated only by a few molecular layers close to the surface. The generation of sum-frequency light is enhanced when the infrared light is resonant with an interfacial molecular vibration. As a result, the SFG technique provides a highly surface-specific vibrational spectrum of the top molecular layers of aqueous solutions. Although the water SFG spectrum contains a wealth of information about the interfacial structure and the present interactions, assigning intensity changes to ion pairing is not unambiguous. For this reason we focus on studies that directly report ions.

For a solution of Na_2SO_4 in contact with a positively charged CaF_2 surface, strong evidence was found for the formation of CIPs between Ca^{2+} ions of the surface and SO_4^{2-} ions of the solution.[8] These CIPs were observed by probing the S−O stretch modes of SO_4^{2-} ions in a combined IR/Raman/SFG study. Scheu et al.[117] used SFG scattering to study the properties of interfacial anions, cations, and water molecules at the surface of a charged nanodroplet surface in water. The droplets were covered with a dilute surfactant layer of an amphiphile ion (dodecyl sulfate), giving rise to a surface charge of 3.7 $\mu C/cm^2$ and corresponding to a potential at the diffuse double layer of −112 mV. Upon addition of 100 *m* MA_nCl salt (Me_4Cl, Et_4Cl, Pr_4Cl, and Bu_4Cl), the surface charge and amount of water orientation were observed to be reduced, pointing at the formation of ion pairs of tetraalkylammonium ions and sulfate groups of the dodecyl surfactant molecules. SFG spectroscopy has also been used to study the interaction between Mg^{2+} ions and palmitic acid at a water−air interface. By probing the C═O stretch vibration of protonated palmitic acid and the symmetric CO_2^- carboxylate stretch vibration of deprotonated palmitic acid, it was found that Mg^{2+} enhances the amount of deprotonation by forming a tight contact ion pair with the carboxylate group of the deprotonated species. By use of SFG, it has also been shown that Ca^{2+} ions strongly bind to the phosphate groups of a monolayer of dipalmitoylphosphatidylcholine (DPPC) on water.[118]

Specific binding of cations to carboxylate and phosphate groups leads to a screening of the negative charges of the biomolecule, which can thereby strongly influence the conformation and function of the biomolecule. SFG spectroscopy has been used to study the association of β-lactoglobulin with cations.[119] In this study, water, amide I, and carboxylate vibrational stretch modes were probed. Together with ellipsometric film thickness measurements and MD simulations, strong evidence for the occurrence of ion pairing of Li^+ and Na^+ ions with aspartate and glutamate carboxylates was found.

Ion-pairing interactions of dissolved anions with proteins and other water-soluble macromolecules have been discussed in a review by Zhang and Cremer.[120] Their review discusses interactions of Hofmeister anions and osmolytes (urea, trimethylamine *N*-oxide) with uncharged polymers, polypeptides, and proteins based on data obtained from vibrational sum frequency spectroscopy and from methods that monitor the hydrophobic collapse of thermoresponsive polymers and peptides as well as aggregation of proteins. The anion binding affinity to the protein backbone is most significant for weakly hydrated, soft (polarizable) anions (I^-, SCN^-, ClO_4^-), with the binding site being identified as a combination of polar amide group and adjacent α-carbon.[121] In comparison with anions, backbone/cation interactions are much weaker.[122] Complementary to the experiments described in the review by Zhang and Cremer,[120] anion and osmolyte interactions with poly(*N*-isopropylacrylamide),[123−125] model amide compounds,[123,126] and amino acids[127] have been recently investigated with molecular simulations and have been discussed in relation to conformational changes of (bio)macromolecules.

Ion pairs are also formed between particular alkali cations and anionic groups on polyelectrolytes, as shown in Figure 10. This figure illustrates how strongly and weakly hydrated cations can have remarkably different effects on the properties of a polymer-functionalized surface. The polymer layer in this example is a diblock copolymer end-grafted with its electrically neutral block to a hydroxylated silica surface, while its charged polyelectrolyte block is exposed to an aqueous solution. Alkali cations act as counterions, neutralizing the electrically charged methacrylic acid (MAA) block in contact with the aqueous solution. At sufficiently high polymer grafting density of the brush, Li^+ and Na^+ form stable bridges between $-CO_2^-$ groups on neighboring chains, while bridging is significantly weaker with K^+, Rb^+, and Cs^+. Interestingly, this observation leads to a 5-fold difference in osmotic compressibility of the polymer layer when Na^+ and K^+ are compared.[128] The observed type of ion-specific mechanical response is important in understanding and designing bioengineered material surfaces with tailored adhesive, wetting, or lubrication properties.

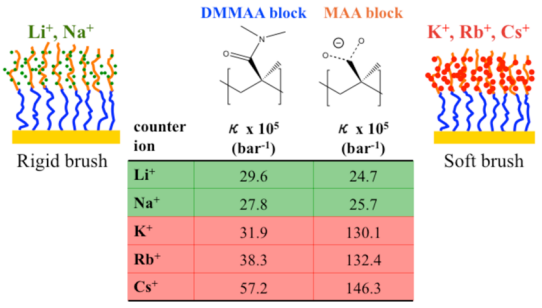

counter ion	κ x 10^5 (bar^{-1})	κ x 10^5 (bar^{-1})
Li^+	29.6	24.7
Na^+	27.8	25.7
K^+	31.9	130.1
Rb^+	38.3	132.4
Cs^+	57.2	146.3

Figure 10. Osmotic compressibility of the *N*,*N*′-dimethylmethylacrylamide (DMMAA) and methacrylic acid (MAA) blocks of a diblock copolymer brush at the interface with water. Different counterions (green and red spheres) neutralize the polyelectrolyte MAA block at the interface with bulk water. Li^+ and Na^+ counterions participate in $COO^-\cdots M^+\cdots{}^-OOC$ salt bridges, induce lateral chain ordering within the brush, and reduce its osmotic compressibility. K^+, Rb^+, and Cs^+ counterions do not induce strong salt bridging, resulting in a disordered soft brush with significantly larger osmotic compressibility of the MAA block. The data have been obtained from computer simulations with empirical force field models.[128]

Recently, ion-specific effects have been reported for the properties of several polymer-functionalized surfaces. These include stability and swelling of polyelectrolyte multilayers,[129] wettability of polymer-functionalized surfaces,[130] thickness and conformational properties of polyelectrolyte brushes[131,132] and polyzwitterionic brushes,[133] and protein adsorption/desorption ability of poly(sulfobetaine methacrylate) zwitterionic brushes.[134] Control of protein adsorption at polyelectrolyte-functionalized surfaces, but also bacterial killing and release on antimicrobial polymer films, depends critically on ion-pairing interactions. Huang et al.[135] reported reversible switchable polycation brushes based on poly[(trimethylamino)ethyl methacrylate chloride] for contact killing of bacteria. Bacterial release is achieved by ion-pairing interactions of counterions with quarternary ammonium groups of the polymer. Yang et al.[136] studied counterion-specific protein adsorption on poly(ionic

DOI: 10.1021/acs.chemrev.5b00742
Chem. Rev. XXXX, XXX, XXX−XXX

liquid) brushes and reported a coupling between the decrease of counterion osmotic pressure in the brush (counterion release) upon protein adsorption and subsequent binding of the released counterions to the protein, leading to ion-specific effects in protein binding to polyelectrolyte-functionalized surfaces. Part of this specificity derives from the binding of counterions (large anions in this case) to electrically neutral groups on the protein.

7. CONCLUSIONS

In this review, we present an overview of a series of recent studies of the molecular structure and dynamics of hydrated ions in aqueous salt solutions over the past decade. In these studies interactions between ions and between ions and water have been investigated with dielectric relaxation spectroscopy, far-infrared (terahertz) absorption spectroscopy, femtosecond mid-infrared spectroscopy, X-ray absorption spectroscopy, and molecular dynamics simulation methods.

With dielectric relaxation and femtosecond mid-infrared spectroscopy, it is found that for many salt solutions the cations and anions show a cooperative effect on reorientation dynamics of the hydration water. These effects are observed for solutions containing Li^+ and Na^+ cations, halide anions, and carboxylate and phosphate anionic groups. The observation of an increased fraction of water molecules that exhibit a slowing-down in their reorientation points at the formation of solvent-shared ion pairs (SIPs) and solvent-separated ion pairs (2SIPs) where the additional "slow" water molecules are located between the cation and the anion.

Formation of SIPs and 2SIPs is also observed in far-infrared absorption studies, X-ray absorption studies, and molecular dynamics simulations. In addition, these techniques show the presence of directly bound cations and anions, so-called contact ion pairs (CIPs). Specific ion-pairing interactions between particular cations, like Li^+ and Na^+, and anionic carboxylate and phosphate groups likely play an important role for (bio)-molecular systems, as these systems often contain a large number of these anionic groups. Ion-pairing interactions with particular cations lead to screening of the negative charges of these anionic groups, thereby affecting the conformation and thus the functionality of these systems.

Recent studies also showed the occurrence of not only ion pairing but also ion clustering in water. This clustering effect is observed in particular for salt solutions containing relatively weakly hydrated anions like SCN^- and for salt solutions containing hydrophobic cations like tetra-*n*-alkylammonium. For the latter system, clustering/aggregation is observed to depend strongly on the length of the alkyl chains of the ion. With increasing chain length, the hydrophobic interaction between the ions increases and can overcome their Coulomb repulsion.

The results presented in this review demonstrate that ion pairing and ion aggregation are not rare phenomena that occur only in highly concentrated salt solutions of strongly interacting cations and anions. Instead, ion pairing is found to occur for many solutions and interfaces of inorganic salts and biomolecular systems and often already at physiologically relevant concentrations. Thereby, these results show that the conventional picture of a salt solution as a statistical mixture of hydrated ions should be refined and that ion-pairing effects play a crucial role in the dynamics of water and the conformation and functioning of (bio)molecular systems in contact with water. With the increasing level of sophistication of experimental methods and simulation models, future progression of the field will contribute to understanding the implications of ion pairing and nonadditive ion effects[137] on the interfacial properties of ions and water and the conformational preferences and stability of biomolecules.

AUTHOR INFORMATION

Corresponding Author

*E-mail vandervegt@csi.tu-darmstadt.de.

Notes

The authors declare no competing financial interest.

Biographies

Nico van der Vegt was born on November 14, 1970, in Raalte, The Netherlands. He received his Ph.D. in chemical engineering from the University of Twente, The Netherlands, in 1998. From 1998 to 2002 he was a lecturer at the University of Twente. From 2002 to 2003 he worked as a postdoc in the group of Professor Dr. Wilfred van Gunsteren at ETH, Zürich, Switzerland. In 2003 he became a group leader at the Max Planck Institute for Polymer Research in Mainz, Germany, heading the group Computational Chemistry and Molecular Simulation. He became full professor of physical chemistry at Technische Universität Darmstadt, Germany, in 2009. His research focuses on the physical fundamentals of aqueous solvation, osmolyte and specific ion effects in soft matter systems, interfacial fluid properties, and development of multiscale simulation methods.

Kristoffer Haldrup obtained his Ph.D. from the Niels Bohr Institute in 2007, after doing his thesis work at the Risø National Laboratory. He then joined the Danish Excellence Center of molecular movies as a postdoc for three years, before moving to Chicago to work with the group of Lin X. Chen as a Villum fellow for a year. Coming back to Denmark on a Carlsberg grant, he rejoined the molecular movies group in the physics department at the Technical University of Denmark (DTU) and in this period also began to shift his focus to investigations of the solvent as a participant in photochemical reaction, not just a spectator. He is now a senior scientist in the physics department and is trying to shed light on the very first, subpicosecond steps in solute−solvent interactions in photochemical reactions by utilizing XFEL sources for investigations of ultrafast structural dynamics.

Sylvie Roke obtained B.Sc. and M.Sc. degrees with highest honors in chemistry (2000) and physics (2000) from Utrecht University and a Ph.D. in natural sciences from Leiden University (2004, highest honors). In 2005 she was awarded an independent research group leader (W2) position from the Max Planck Society. In 2011 she moved to EPFL, where she holds the Juli Jacobi chair in photomedicine. She received the Minerva Prize (2006), the Hertha Sponer Prize (2008), an ERC Starting Grant (2009), and an ERC Consolidator Grant (2014). Her research focuses on understanding aqueous systems, interfaces, soft matter, and biological systems by using a variety of spectroscopic and imaging methods.

Junrong Zheng received his Ph.D. from Stanford University in 2007. After working as a postdoctoral researcher at Stanford University and a visiting scholar at UC Berkeley, he joined Rice University as an assistant professor of chemistry in 2009. He moved to Peking University as a professor between 2015 and 2016. His current research focuses on developing novel spectroscopic tools for determination of molecular structures and dynamics and on femtomachining methods for medical and electronic applications.

Mikael Lund has been, since 2012, an associate professor at the division of theoretical chemistry at Lund University, Sweden. He finished his Ph.D. in 2007 within the topic of protein−protein interactions and subsequently joined the group of Pavel Jungwirth in Prague to do postdoctoral studies of ion-specific effects. His research focuses on biomolecular interactions and how these are influenced by solution

DOI: 10.1021/acs.chemrev.5b00742
Chem. Rev. XXXX, XXX, XXX−XXX

conditions, such as macromolecular density, pH, salt concentration, and type.

Huib Johan Bakker was born on March 2, 1965, in Haarlem, The Netherlands. He did his Ph.D. studies in the group of Professor Dr. Ad Lagendijk at the FOM Institute for Atomic and Molecular Physics (AMOLF). From 1991 to 1994 he worked as a postdoc in the group of Professor Dr. Heinrich Kurz at the Institute of Semiconductor Electronics, Technical University of Aachen, Germany. In 1995 he became a group leader at AMOLF, heading the group on ultrafast spectroscopy. Research work of this group includes spectroscopic study of the structure and ultrafast dynamics of water interacting with ions and (bio)molecular systems and study of the mechanism of proton transfer in aqueous media. In 2001 he became a full professor of physical chemistry at the University of Amsterdam, The Netherlands, and in 2003 he became department head in molecular nanophysics at FOM-AMOLF. In 2004, he received the gold medal of the Royal Netherlands Chemical Society for his work on the ultrafast dynamics of aqueous systems. Since February 1, 2016, he has been director of AMOLF.

ACKNOWLEDGMENTS

This review was initiated during the Nordita (Nordic Institute for Theoretical Physics) scientific program "Water - the Most Anomalous Liquid". Additional financial support for this program was provided by the Royal Swedish Academy of Sciences through its Nobel Institutes for Physics and Chemistry, by the Swedish Research Council, and by the Department of Physics at Stockholm University. H.J.B. acknowledges support of the Stichting voor Fundamenteel Onderzoek der Materie (FOM), which is financially supported by the Nederlandse Organisatie voor Wetenschappelijk Onderzoek (NWO). N.F.A.v.d.V. acknowledges funding by the LOEWE project iNAPO of the Hessen State Ministry of Higher Education, Research and the Arts. N.F.A.v.d.V. acknowledges F. Taherian for her help with editing the references.

REFERENCES

(1) Bernal, J. D.; Fowler, R. H. A theory of water and ionic solution, with particular reference to hydrogen and hydroxyl ions. *J. Chem. Phys.* **1933**, *1*, 515−548.
(2) Ohtaki, H.; Radnai, T. Structure and dynamics of hydrated ions. *Chem. Rev.* **1993**, *93*, 1157−1204.
(3) Marcus, Y. Effect of ions on the structure of water: structure making and breaking. *Chem. Rev.* **2009**, *109*, 1346−1370.
(4) Marcus, Y.; Hefter, G. Ion pairing. *Chem. Rev.* **2006**, *106*, 4585−4621.
(5) Mason, P. E.; Neilson, G. W.; Enderby, J. E.; Saboungi, M.-L.; Dempsey, C. E.; MacKerell, A. D., Jr.; Brady, J. W. The structure of aqueous guanidinium chloride solutions. *J. Am. Chem. Soc.* **2004**, *126*, 11462−11470.
(6) Shih, O.; England, A. H.; Dallinger, G. C.; Smith, J. W.; Duffey, K. C.; Cohen, R. C.; Prendergast, D.; Saykally, R. J. Cation-cation contact pairing in water: Guanidinium. *J. Chem. Phys.* **2013**, *139*, 035104.
(7) Geissler, P. L.; Dellago, C.; Chandler, D. Kinetic pathways of ion pair dissociation in water. *J. Phys. Chem. B* **1999**, *103*, 3706−3710.
(8) Jubb, A. M.; Allen, H. C. Sulfate adsorption at the buried fluorite-solution interface revealed by vibrational sum frequency generation spectroscopy. *J. Phys. Chem. C* **2012**, *116*, 9085−9091.
(9) Tobias, D. J.; Stern, A. C.; Baer, M. D.; Levin, Y.; Mundy, C. J. Simulation and theory of ions at atmospherically relevant aqueous liquid-air interfaces. *Annu. Rev. Phys. Chem.* **2013**, *64*, 339−359.
(10) Johnson, C. M.; Baldelli, S. Vibrational sum frequency spectroscopy studies of the influence of solutes and phospholipids at vapor/water interfaces relevant to biological and environmental systems. *Chem. Rev.* **2014**, *114*, 8416−8446.
(11) Buchner, R.; Capewell, S. G.; Hefter, G.; May, P. M. Ion-pair and solvent relaxation processes in aqueous Na_2SO_4 solutions. *J. Phys. Chem. B* **1999**, *103*, 1185−1192.
(12) Buchner, R.; Chen, T.; Hefter, G. Complexity in "simple" electrolyte solutions: Ion pairing in $MgSO_4$(aq). *J. Phys. Chem. B* **2004**, *108*, 2365−2375.
(13) Tielrooij, K. J.; Garcia-Araez, N.; Bonn, M.; Bakker, H. J. Cooperativity in ion hydration. *Science* **2010**, *328*, 1006−1009.
(14) van der Post, S. T.; Scheidelaar, S.; Bakker, H. J. Water dynamics in aqueous solutions of tetra-n-alkylammonium salts: Hydrophobic and coulomb interactions disentangled. *J. Phys. Chem. B* **2013**, *117*, 15101−15110.
(15) Bian, H. T.; Wen, X. W.; Li, J. B.; Chen, H. L.; Han, S. Z.; Sun, X. Q.; Song, J. A.; Zhuang, W.; Zheng, J. R. Ion clustering in aqueous solutions probed with vibrational energy transfer. *Proc. Natl. Acad. Sci. U. S. A.* **2011**, *108*, 4737−4742.
(16) Chen, H. L.; Wen, X. W.; Li, J. B.; Zheng, J. R. Molecular distances determined with resonant vibrational energy transfers. *J. Phys. Chem. A* **2014**, *118*, 2463−2469.
(17) Chen, T.; Hefter, G.; Buchner, R. Ion association and hydration in aqueous solutions of nickel(II) and cobalt(II) sulfate. *J. Solution Chem.* **2005**, *34*, 1045−1066.
(18) Akilan, C.; Hefter, G.; Rohman, N.; Buchner, R. Ion association and hydration in aqueous solutions of copper(II) sulfate from 5 to 65 degrees C by dielectric spectroscopy. *J. Phys. Chem. B* **2006**, *110*, 14961−14970.
(19) Guardia, E.; Rey, R.; Padro, J. A. Potential of mean force by constrained molecular-dynamics - a sodium-chloride ion-pair in water. *Chem. Phys.* **1991**, *155*, 187−195.
(20) Zhu, S. B.; Robinson, G. W. Molecular-dynamics computer-simulation of an aqueous NaCl solution - structure. *J. Chem. Phys.* **1992**, *97*, 4336−4348.
(21) Pratt, L. R.; Hummer, G.; Garcia, A. E. Ion-pair potentials-of-mean-force in water. *Biophys. Chem.* **1994**, *51*, 147−165.
(22) Smith, D. E.; Dang, L. X. Computer-simulations of NaCl association in polarizable water. *J. Chem. Phys.* **1994**, *100*, 3757−3766.
(23) Lyubartsev, A. P.; Laaksonen, A. Concentration effects in aqueous NaCl solutions. A molecular dynamics simulation. *J. Phys. Chem.* **1996**, *100*, 16410−16418.
(24) Koneshan, S.; Rasaiah, J. C. Computer simulation studies of aqueous sodium chloride solutions at 298 and 683 K. *J. Chem. Phys.* **2000**, *113*, 8125−8137.
(25) Jagoda-Cwiklik, B.; Vacha, R.; Lund, M.; Srebro, M.; Jungwirth, P. Ion pairing as a possible clue for discriminating between sodium and potassium in biological and other complex environments. *J. Phys. Chem. B* **2007**, *111*, 14077−14079.
(26) Hess, B.; van der Vegt, N. F. A. Cation specific binding with protein surface charges. *Proc. Natl. Acad. Sci. U. S. A.* **2009**, *106*, 13296−13300.
(27) Heyda, J.; Lund, M.; Oncak, M.; Slavicek, P.; Jungwirth, P. Reversal of Hofmeister ordering for pairing of NH_4^+ vs alkylated ammonium cations with halide anions in water. *J. Phys. Chem. B* **2010**, *114*, 10843−10852.
(28) Ganguly, P.; Schravendijk, P.; Hess, B.; van der Vegt, N. F. A. Ion pairing in aqueous electrolyte solutions with biologically relevant anions. *J. Phys. Chem. B* **2011**, *115*, 3734−3739.
(29) Nguyen, P. T. M.; Nguyen, V. T.; Annapureddy, H. V. R.; Dang, L. X.; Do, D. D. Thermodynamics and kinetics of Na^+/K^+-formate ion pairs association in polarizable water: A molecular dynamics study. *Chem. Phys. Lett.* **2012**, *554*, 90−95.
(30) Annapureddy, H. V. R.; Dang, L. X. Molecular mechanism of specific ion interactions between alkali cations and acetate anion in aqueous solution: A molecular dynamics study. *J. Phys. Chem. B* **2012**, *116*, 7492−7498.
(31) Stirnemann, G.; Wernersson, E.; Jungwirth, P.; Laage, D. Mechanisms of acceleration and retardation of water dynamics by ions. *J. Am. Chem. Soc.* **2013**, *135*, 11824−11831.

DOI: 10.1021/acs.chemrev.5b00742
Chem. Rev. XXXX, XXX, XXX−XXX

(32) Vazdar, M.; Uhlig, F.; Jungwirth, P. Like-charge ion pairing in water: An ab initio molecular dynamics study of aqueous guanidinium cations. *J. Phys. Chem. Lett.* **2012**, *3*, 2021−2024.
(33) Vila Verde, A.; Lipowsky, R. Cooperative slowdown of water rotation near densely charged ions is intense but short-ranged. *J. Phys. Chem. B* **2013**, *117*, 10556−10566.
(34) Zhang, Q.; Zhang, R. T.; Zhao, Y.; Li, H. H.; Gao, Y. Q.; Zhuang, W. Pairing preferences of the model mono-valence mono-atomic ions investigated by molecular simulation. *J. Chem. Phys.* **2014**, *140*, 184504.
(35) Pokapanich, W.; Ottosson, N.; Svensson, S.; Öhrwall, G.; Winter, B.; Björneholm, O. Bond breaking, electron pushing, and proton pulling: Active and passive roles in the interaction between aqueous ions and water as manifested in the O 1s Auger decay. *J. Phys. Chem. B* **2012**, *116*, 3−8.
(36) Bowron, D. T.; Diaz Moreno, S. Using synchrotron X-ray and neutron methods to investigate structural aspects of metal ion solvation and solution structure: An approach using empirical potential structure refinement. *Coord. Chem. Rev.* **2014**, *277-278*, 2−14.
(37) Lee, P. A.; Citrin, P. H.; Eisenberger, P.; Kincaid, B. M. Extended X-ray absorption fine structure—its strengths and limitations as a structural tool. *Rev. Mod. Phys.* **1981**, *53*, 769−806.
(38) Stern, E. A. Number of relevant points independent points in X-ray absorption fine-structure spectra. *Phys. Rev. B: Condens. Matter Mater. Phys.* **1993**, *48*, 9825−9827.
(39) Haldrup, K.; Christensen, M.; Nielsen, M. M. Analysis of time-resolved X-ray scattering data from solution-state systems. *Acta Crystallogr., Sect. A: Found. Crystallogr.* **2010**, *66*, 261−269.
(40) Fulton, J. L.; Heald, S. M.; Badyal, Y. S.; Simonson, J. M. Understanding the effects of concentration on the solvation structure of Ca^{2+} in aqueous solution. I: The perspective on local structure from EXAFS and XANES. *J. Phys. Chem. A* **2003**, *107*, 4688−4696.
(41) Enderby, J. E. Ion solvation via neutron-scattering. *Chem. Soc. Rev.* **1995**, *24*, 159−168.
(42) Badyal, Y. S.; Barnes, A. C.; Cuello, G. J.; Simonson, J. M. Understanding the effects of concentration on the solvation structure of Ca^{2+} in aqueous solutions. II: Insights into longer range order from neutron diffraction isotope substitution. *J. Phys. Chem. A* **2004**, *108*, 11819−11827.
(43) Soper, A. K. Tests of the empirical potential structure refinement method and a new method of application to neutron diffraction data on water. *Mol. Phys.* **2001**, *99*, 1503−1516.
(44) Soper, A. K. Partial structure factors from disordered materials diffraction data: An approach using empirical potential structure refinement. *Phys. Rev. B: Condens. Matter Mater. Phys.* **2005**, *72*, No. 104204.
(45) Diaz-Moreno, S.; Ramos, S.; Bowron, D. T. Solvation structure and ion complexation of La^{3+} in a 1 molal aqueous solution of lanthanum chloride. *J. Phys. Chem. A* **2011**, *115*, 6575−6581.
(46) Megyes, T.; Balint, S.; Peter, E.; Grosz, T.; Bako, I.; Krienke, H.; Bellissent-Funel, M.-C. Solution structure of $NaNO_3$ in water: Diffraction and molecular dynamics simulation study. *J. Phys. Chem. B* **2009**, *113*, 4054−4064.
(47) Pham, V. T.; Fulton, J. L. Ion-pairing in aqueous $CaCl_2$ and RbBr solutions: Simultaneous structural refinement of XAFS and XRD data. *J. Chem. Phys.* **2013**, *138*, 044201.
(48) Sharma, V.; Böhm, F.; Seitz, M.; Schwaab, G.; Havenith, M. From solvated ions to ion-pairing: a THz study of lanthanum (III) hydration. *Phys. Chem. Chem. Phys.* **2013**, *15*, 8383−8391.
(49) Sharma, V.; Böhm, F.; Schwaab, G.; Havenith, M. The low frequency motions of solvated Mn (ii) and Ni (ii) ions and their halide complexes. *Phys. Chem. Chem. Phys.* **2014**, *16*, 25101−25110.
(50) Böhm, F.; Sharma, V.; Schwaab, G.; Havenith, M. The low frequency modes of solvated ions and ion pairs in aqueous electrolyte solutions: iron (II) and iron (III) chloride. *Phys. Chem. Chem. Phys.* **2015**, *17*, 19582−19591.
(51) Thürmer, S.; Seidel, R.; Eberhardt, W.; Bradforth, S. E.; Winter, B. Ultrafast hybridization screening in Fe^{3+} aqueous solution. *J. Am. Chem. Soc.* **2011**, *133*, 12528−12535.
(52) Wachter, W.; Fernandez, S.; Buchner, R.; Hefter, G. Ion association and hydration in aqueous solutions of LiCl and Li_2SO_4 by dielectric spectroscopy. *J. Phys. Chem. B* **2007**, *111*, 9010−9017.
(53) Fedotova, M. V.; Kruchinin, S. E.; Rahman, H. M. A.; Buchner, R. Features of ion hydration and association in aqueous rubidium fluoride solutions at ambient conditions. *J. Mol. Liq.* **2011**, *159*, 9−17.
(54) Eiberweiser, A.; Buchner, R. Ion-pair or ion-cloud relaxation? On the origin of small-amplitude low-frequency relaxations of weakly associating aqueous electrolytes. *J. Mol. Liq.* **2012**, *176*, 52−59.
(55) van der Post, S. T.; Bakker, H. J. The combined effect of cations and anions on the dynamics of water. *Phys. Chem. Chem. Phys.* **2012**, *14*, 6280−6288.
(56) Fennell, C. J.; Bizjak, A.; Vlachy, V.; Dill, K. A. Ion pairing in molecular simulations of aqueous alkali halide solutions. *J. Phys. Chem. B* **2009**, *113*, 6782−6791.
(57) Collins, K. D. Charge density-dependent strength of hydration and biological structure. *Biophys. J.* **1997**, *72*, 65−76.
(58) Collins, K. D. Ions from the Hofmeister series and osmolytes: effects on proteins in solution and in the crystallization process. *Methods* **2004**, *34*, 300−311.
(59) Kirkwood, J. G.; Buff, F. P. The statistical mechanical theory of solutions 1. *J. Chem. Phys.* **1951**, *19*, 774−777.
(60) Ben-Naim, A. *Molecular Theory of Solutions*; Oxford University Press: New York, 2006; p 112.
(61) Krüger, P.; Schnell, S. K.; Bedeaux, D.; Kjelstrup, S.; Vlugt, T. J.; Simon, J.-M. Kirkwood−Buff integrals for finite volumes. *J. Phys. Chem. Lett.* **2013**, *4*, 235−238.
(62) Ganguly, P.; van der Vegt, N. F. A. Convergence of sampling Kirkwood−Buff integrals of aqueous solutions with molecular dynamics simulations. *J. Chem. Theory Comput.* **2013**, *9*, 1347−1355.
(63) Weerasinghe, S.; Smith, P. E. A Kirkwood−Buff derived force field for sodium chloride in water. *J. Chem. Phys.* **2003**, *119*, 11342−11349.
(64) Weerasinghe, S.; Smith, P. E. A Kirkwood-Buff derived force field for the simulation of aqueous guanidinium chloride solutions. *J. Chem. Phys.* **2004**, *121*, 2180−2186.
(65) Klasczyk, B.; Knecht, V. Kirkwood−Buff derived force field for alkali chlorides in simple point charge water. *J. Chem. Phys.* **2010**, *132*, 024109.
(66) Gee, M. B.; Cox, N. R.; Jiao, Y.; Bentenitis, N.; Weerasinghe, S.; Smith, P. E. A Kirkwood-Buff derived force field for aqueous alkali halides. *J. Chem. Theory Comput.* **2011**, *7*, 1369−1380.
(67) Fyta, M.; Netz, R. R. Ionic force field optimization based on single-ion and ion-pair solvation properties: Going beyond standard mixing rules. *J. Chem. Phys.* **2012**, *136*, 124103.
(68) Mamatkulov, S.; Fyta, M.; Netz, R. R. Force fields for divalent cations based on single-ion and ion-pair properties. *J. Chem. Phys.* **2013**, *138*, 024505.
(69) Schnell, S. K.; Englebienne, P.; Simon, J.-M.; Krüger, P.; Balaji, S. P.; Kjelstrup, S.; Bedeaux, D.; Bardow, A.; Vlugt, T. J. How to apply the Kirkwood−Buff theory to individual species in salt solutions. *Chem. Phys. Lett.* **2013**, *582*, 154−157.
(70) Robinson, R. A.; Stokes, R. H. *Electrolyte Solutions*, 2nd revised ed.; Dover Publications: Mineola, NY, 2002; pp 483−485.
(71) Robinson, R. A.; Harned, H. S. Some aspects of the thermodynamics of strong electrolytes from electromotive force and vapor pressure measurements. *Chem. Rev.* **1941**, *28*, 419−476.
(72) Tromans, A.; May, P. M.; Hefter, G.; Sato, T.; Buchner, R. Ion pairing and solvent relaxation processes in aqueous solutions of sodium malonate and sodium succinate. *J. Phys. Chem. B* **2004**, *108*, 13789−13795.
(73) Capewell, S. G.; Buchner, R.; Hefter, G.; May, P. M. Dielectric relaxation of aqueous Na_2CO_3 solutions. *Phys. Chem. Chem. Phys.* **1999**, *1*, 1933−1937.
(74) Rahman, H. M. A.; Hefter, G.; Buchner, R. Hydration of formate and acetate ions by dielectric relaxation spectroscopy. *J. Phys. Chem. B* **2012**, *116*, 314−323.
(75) Rahman, H. M. A.; Buchner, R. Hydration and sodium-ion binding of trifluoroacetate in aqueous solution. *J. Mol. Liq.* **2012**, *176*, 93−100.

DOI: 10.1021/acs.chemrev.5b00742
Chem. Rev. XXXX, XXX, XXX−XXX

(76) Van der Post, S. T.; Hunger, J.; Bonn, M.; Bakker, H. J. Observation of water separated ion-pairs between cations and phospholipid headgroups. *J. Phys. Chem. B* **2014**, *118*, 4397−4403.
(77) Pastorczak, M.; van der Post, S. T.; Bakker, H. J. Cooperative hydration of carboxylate groups with alkali cations. *Phys. Chem. Chem. Phys.* **2013**, *15*, 17767−17770.
(78) Aziz, E. F.; Ottosson, N.; Eisebitt, S.; Eberhardt, W.; Jagoda-Cwiklik, B.; Vácha, R.; Jungwirth, P.; Winter, B. Cation-specific interactions with carboxylate in amino acid and acetate aqueous solutions: X-ray absorption and ab initio calculations. *J. Phys. Chem. B* **2008**, *112*, 12567−12570.
(79) Hajari, T.; Ganguly, P.; van der Vegt, N. F. A. Enthalpy-entropy of cation association with the acetate anion in water. *J. Chem. Theory Comput.* **2012**, *8*, 3804−3809.
(80) Debye, P.; Huckel, E. On the theory of electrolytes I. The lowering of the freezing point and related occurrences. *Phys. Z.* **1923**, *24*, 185−206.
(81) Barthel, J.; Krienke, H.; Kunz, W. *Physical Chemistry of Electrolyte Solutions: Modern Aspects*; Springer: New York, 1998.
(82) Pytkowicz, R. M. *Activity Coefficients in Electrolyte Solutions*; CRC Press: Boca Raton, FL, 1979; Vol. *1*.
(83) Conway, B. E. *Ionic Hydration in Chemistry and Biophysics*; Elsevier: New York, 1981.
(84) Sherman, D. M.; Collings, M. D. Ion association in concentrated NaCl brines from ambient to supercritical conditions: results from classical molecular dynamics simulations. *Geochem. Trans.* **2002**, *3*, 102−107.
(85) Degreve, L.; da Silva, F. L. B. Structure of concentrated aqueous NaCl solution: A Monte Carlo study. *J. Chem. Phys.* **1999**, *110*, 3070−3078.
(86) Hassan, S. A. Computer simulation of ion cluster speciation in concentrated aqueous solutions at ambient conditions. *J. Phys. Chem. B* **2008**, *112*, 10573−10584.
(87) Chen, A. A.; Pappu, R. V. Quantitative characterization of ion pairing and cluster formation in strong 1:1 electrolytes. *J. Phys. Chem. B* **2007**, *111*, 6469−6478.
(88) Cerreta, M. K.; Berglund, K. A. The Structure of aqueous-solutions of some dihydrogen ortho-phosphates by laser raman-spectroscopy. *J. Cryst. Growth* **1987**, *84*, 577−588.
(89) Rusli, I. T.; Schrader, G. L.; Larson, M. A. Raman spectroscopic study of $NaNO_3$ solution system - solute clustering in supersaturated solutions. *J. Cryst. Growth* **1989**, *97*, 345−351.
(90) Mason, P. E.; Dempsey, C. E.; Neilson, G. W.; Brady, J. W. Nanometer-scale ion aggregates in aqueous electrolyte solutions: Guanidinium sulfate and guanidinium thiocyanate. *J. Phys. Chem. B* **2005**, *109*, 24185−24196.
(91) Sedlák, M. Large-scale supramolecular structure in solutions of low molar mass compounds and mixtures of liquids: I. Light scattering characterization. *J. Phys. Chem. B* **2006**, *110*, 4329−4338.
(92) Sedlák, M. Large-scale supramolecular structure in solutions of low molar mass compounds and mixtures of liquids: II. Kinetics of the formation and long-time stability. *J. Phys. Chem. B* **2006**, *110*, 4339−4345.
(93) Fitter, J.; Gutberlet, T.; Katsaras, J. *Neutron Scattering in Biology: Techniques and Applications*; Springer: Berlin and Heidelberg, Germany, 2006; DOI: 10.1007/3-540-29111-3.
(94) Berne, B.; Pecora, R. *Dynamic Light Scattering: With Applications to Chemistry, Biology, and Physics*; Wiley: New York, 1976.
(95) Chen, H. L.; Wen, X. W.; Guo, X. M.; Zheng, J. R. Intermolecular vibrational energy transfers in liquids and solids. *Phys. Chem. Chem. Phys.* **2014**, *16*, 13995−14014.
(96) Li, J. B.; Bian, H. T.; Chen, H. L.; Wen, X. W.; Hoang, B. T.; Zheng, J. R. Ion association in aqueous solutions probed through vibrational energy transfers among cation, anion, and water molecules. *J. Phys. Chem. B* **2013**, *117*, 4274−4283.
(97) Bian, H. T.; Chen, H. L.; Zhang, Q.; Li, J. B.; Wen, X. W.; Zhuang, W.; Zheng, J. R. Cation effects on rotational dynamics of anions and water molecules in alkali (Li^+, Na^+, K^+, Cs^+) Thiocyanate (SCN^-) aqueous solutions. *J. Phys. Chem. B* **2013**, *117*, 7972−7984.
(98) Li, J. B.; Bian, H. T.; Wen, X. W.; Chen, H. L.; Yuan, K. J.; Zheng, J. R. Probing Ion/Molecule Interactions in Aqueous Solutions with Vibrational Energy Transfer. *J. Phys. Chem. B* **2012**, *116*, 12284−12294.
(99) Bian, H. T.; Li, J. B.; Zhang, Q.; Chen, H. L.; Zhuang, W.; Gao, Y. Q.; Zheng, J. R. Ion segregation in aqueous solutions. *J. Phys. Chem. B* **2012**, *116*, 14426−14432.
(100) Bian, H. T.; Chen, H. L.; Li, J. B.; Wen, X. W.; Zheng, J. R. Nonresonant and resonant mode-specific intermolecular vibrational energy transfers in electrolyte aqueous solutions. *J. Phys. Chem. A* **2011**, *115*, 11657−11664.
(101) Lund, M.; Jagoda-Cwiklik, B.; Woodward, C. E.; Vácha, R.; Jungwirth, P. Dielectric interpretation of specificity of ion pairing in water. *J. Phys. Chem. Lett.* **2010**, *1*, 300−303.
(102) Kim, S.; Kim, H.; Choi, J. H.; Cho, M. Ion aggregation in high salt solutions: Ion network versus ion cluster. *J. Chem. Phys.* **2014**, *141*, 124510.
(103) Sun, Z.; Zhang, W. K.; Ji, M. B.; Hartsock, R.; Gaffney, K. J. Contact ion pair formation between hard acids and soft bases in aqueous solutions observed with 2DIR spectroscopy. *J. Phys. Chem. B* **2013**, *117*, 15306−15312.
(104) Zhang, Q.; Xie, W. J.; Bian, H. T.; Gao, Y. Q.; Zheng, J. R.; Zhuang, W. Microscopic origin of the deviation from Stokes-Einstein behavior observed in dynamics of the KSCN aqueous solutions: A MD simulation study. *J. Phys. Chem. B* **2013**, *117*, 2992−3004.
(105) Marcus, Y. Tetraalkylammonium ions in aqueous and non-aqueous solutions. *J. Solution Chem.* **2008**, *37*, 1071−1098.
(106) Polydorou, N. G.; Wicks, J. D.; Turner, J. Z. Hydrophobic interaction of tetrapropylammonium ions in water: A neutron diffraction and reverse Monte Carlo study. *J. Chem. Phys.* **1997**, *107*, 197−204.
(107) Buchner, R.; Holzl, C.; Stauber, J.; Barthel, J. Dielectric spectroscopy of ion-pairing and hydration in aqueous tetra-n-alkylammonium halide solutions. *Phys. Chem. Chem. Phys.* **2002**, *4*, 2169−2179.
(108) Huang, N.; Schlesinger, D.; Nordlund, D.; Huang, C.; Tyliszczak, T.; Weiss, T. M.; Acremann, Y.; Pettersson, L. G. M.; Nilsson, A. Microscopic probing of the size dependence in hydrophobic solvation. *J. Chem. Phys.* **2012**, *136*, 074507.
(109) Skinner, J. L.; Pieniazek, P. A.; Gruenbaum, S. M. Vibrational spectroscopy of water at interfaces. *Acc. Chem. Res.* **2012**, *45*, 93−100.
(110) Wong, D. B.; Giammanco, C. H.; Fenn, E. E.; Fayer, M. D. Dynamics of isolated water molecules in a sea of ions in a room temperature ionic liquid. *J. Phys. Chem. B* **2013**, *117*, 623−635.
(111) Lindman, B.; Wennerstrom, H.; Forsen, S. A bromine-79 nuclear magnetic resonance study of the structure of aqueous solutions of mono-, di-, and trialkylammonium bromides. *J. Phys. Chem.* **1970**, *74*, 754−760.
(112) Lindblom, G.; Lindman, B. Interaction between halide ions and amphiphilic organic cations in aqueous solutions studied by nuclear quadrupole relaxation. *J. Phys. Chem.* **1973**, *77*, 2531−2537.
(113) Long, J. A.; Rankin, B. M.; Ben-Amotz, D. Micelle structure and hydrophobic hydration. *J. Am. Chem. Soc.* **2015**, *137*, 10809−10815.
(114) McCormick, A.; Bell, A.; Radke, C. Evidence from alkali-metal NMR spectroscopy for ion pairing in alkaline silicate solutions. *J. Phys. Chem.* **1989**, *93*, 1733−1737.
(115) Bjerrum, N. J. *Untersuchungen über Ionenassoziation*; A. F. Høst: Copenhagen, Denmark, 1926.
(116) Perera, G. S.; Nettles, C. B.; Zhou, Y.; Zou, S.; Hollis, T. K.; Zhang, D. Direct observation of ion pairing at the liquid/solid interfaces by surface enhanced Raman spectroscopy. *Langmuir* **2015**, *31*, 8998−9005.
(117) Scheu, R.; Chen, Y. X.; Subinya, M.; Roke, S. Stern layer formation induced by hydrophobic interactions: A molecular level study. *J. Am. Chem. Soc.* **2013**, *135*, 19330−19335.
(118) Casillas-Ituarte, N. N.; Chen, X.; Castada, H.; Allen, H. C. Na+ and Ca2+ effect on the hydration and orientation of the phosphate group of DPPC at air− water and air− hydrated silica interfaces. *J. Phys. Chem. B* **2010**, *114*, 9485−9495.

DOI: 10.1021/acs.chemrev.5b00742
Chem. Rev. XXXX, XXX, XXX−XXX

(119) Beierlein, F. R.; Clark, T.; Braunschweig, B.; Engelhardt, K.; Glas, L.; Peukert, W. Carboxylate ion pairing with alkali-metal ions for beta-lactoglobulin and its role on aggregation and interfacial adsorption. *J. Phys. Chem. B* **2015**, *119*, 5505−5517.
(120) Zhang, Y.; Cremer, P. S. Chemistry of Hofmeister anions and osmolytes. *Annu. Rev. Phys. Chem.* **2010**, *61*, 63−83.
(121) Rembert, K. B.; Paterová, J.; Heyda, J.; Hilty, C.; Jungwirth, P.; Cremer, P. S. Molecular mechanisms of ion-specific effects on proteins. *J. Am. Chem. Soc.* **2012**, *134*, 10039−10046.
(122) Okur, H. I.; Kherb, J.; Cremer, P. S. Cations bind only weakly to amides in aqueous solutions. *J. Am. Chem. Soc.* **2013**, *135*, 5062−5067.
(123) Algaer, E. A.; van der Vegt, N. F. A. Hofmeister ion interactions with model amide compounds. *J. Phys. Chem. B* **2011**, *115*, 13781−13787.
(124) Rodriguez-Ropero, F.; van der Vegt, N. F. A. Direct osmolyte−macromolecule interactions confer entropic stability to folded states. *J. Phys. Chem. B* **2014**, *118*, 7327−7334.
(125) Rodríguez-Ropero, F.; van der Vegt, N. F. A. On the urea induced hydrophobic collapse of a water soluble polymer. *Phys. Chem. Chem. Phys.* **2015**, *17*, 8491−8498.
(126) Heyda, J.; Vincent, J. C.; Tobias, D. J.; Dzubiella, J.; Jungwirth, P. Ion specificity at the peptide bond: Molecular dynamics simulations of N-methylacetamide in aqueous salt solutions. *J. Phys. Chem. B* **2010**, *114*, 1213−1220.
(127) Ganguly, P.; Hajari, T.; Shea, J.-E.; van der Vegt, N. F. A. Mutual exclusion of urea and trimethylamine N-oxide from amino acids in mixed solvent environment. *J. Phys. Chem. Lett.* **2015**, *6*, 581−585.
(128) Rodríguez-Ropero, F.; van der Vegt, N. F. A. Ionic specific effects on the structure, mechanics and interfacial softness of a polyelectrolyte brush. *Faraday Discuss.* **2013**, *160*, 297−309.
(129) Volodkin, D.; von Klitzing, R. Competing mechanisms in polyelectrolyte multilayer formation and swelling: Polycation−polyanion pairing vs. polyelectrolyte−ion pairing. *Curr. Opin. Colloid Interface Sci.* **2014**, *19*, 25−31.
(130) Liao, K.-S.; Fu, H.; Wan, A.; Batteas, J. D.; Bergbreiter, D. E. Designing surfaces with wettability that varies in response to solute identity and concentration. *Langmuir* **2009**, *25*, 26−28.
(131) Moya, S. E.; Azzaroni, O.; Kelby, T.; Donath, E.; Huck, W. T. Explanation for the apparent absence of collapse of polyelectrolyte brushes in the presence of bulky ions. *J. Phys. Chem. B* **2007**, *111*, 7034−7040.
(132) Willott, J. D.; Murdoch, T. J.; Humphreys, B. A.; Edmondson, S.; Wanless, E. J.; Webber, G. B. Anion-specific effects on the behavior of pH-sensitive polybasic brushes. *Langmuir* **2015**, *31*, 3707−3717.
(133) Matsuoka, H.; Yamakawa, Y.; Ghosh, A.; Saruwatari, Y. Nanostructure and salt effect of zwitterionic carboxybetaine brush at the air/water interface. *Langmuir* **2015**, *31*, 4827−4836.
(134) Wang, T.; Wang, X.; Long, Y.; Liu, G.; Zhang, G. Ion-specific conformational behavior of polyzwitterionic brushes: Exploiting it for protein adsorption/desorption control. *Langmuir* **2013**, *29*, 6588−6596.
(135) Huang, C.-J.; Chen, Y.-S.; Chang, Y. Counterion-activated nanoactuator: reversibly switchable killing/releasing bacteria on polycation brushes. *ACS Appl. Mater. Interfaces* **2015**, *7*, 2415−2423.
(136) Yang, J.; Hua, Z.; Wang, T.; Wu, B.; Liu, G.; Zhang, G. Counterion-specific protein adsorption on polyelectrolyte brushes. *Langmuir* **2015**, *31*, 6078−6084.
(137) Jungwirth, P.; Cremer, P. S. Beyond Hofmeister. *Nat. Chem.* **2014**, *6*, 261−263.

DOI: 10.1021/acs.chemrev.5b00742
Chem. Rev. XXXX, XXX, XXX−XXX